ENVIRONMENTAL CONTROLS ON THE GROWTH OF DUNE-BUILDING GRASSES
AND THE EFFECT OF PLANT MORPHOLOGY ON COASTAL FOREDUNE FORMATION

Theo Jass

A thesis submitted to the faculty at the University of North Carolina at Chapel Hill in partial fulfillment of the requirements for the degree of Master of Science in the Department of Geological Sciences in the School of Arts and Sciences.

Chapel Hill
2015

Approved by:

Laura J. Moore

John F. Bruno

Antonio B. Rodriguez

ABSTRACT

Theo Jass: Environmental Controls on the Growth of Dune-Building Grasses and the Effect of
Plant Morphology on Coastal Foredune Formation
(Under the direction of Laura J. Moore)

Vegetated coastal foredunes protect habitats and infrastructure from storm-driven

flooding. To improve understanding of foredune formation and morphology by quantifying the

relationship between plant growth and position (cross-shore and elevation), I planted and

monitored 180 individuals (*Ammophila breviligulata*, *Spartina patens*, *Uniola paniculata*) on

Hog Island, Virginia.

Growth in all species was correlated with change in elevation, and varied with position in

S. patens and *U. paniculata*. Relationships were most predictive in *A. breviligulata* and *U.

paniculata*. Transplant basal area and lateral spreading was greater at low elevations (340 cm^2,

48%) than at intermediate (95, 17%) or high elevations (107, 20%). I derived allometric scaling

relationships relating longest visible leaf length to basal and frontal area and found that the

empirical ratio of basal-to-frontal area (~0.8, all species) maximized dune height in a

morphodynamic foredune growth model. Model results suggest that plant morphology exerts a

nonlinear control on dune morphology.

To Kirby, I love you.
To my dad, a great man and a great scientist.
To my mom, who took me to the beach to see the dunes in New Jersey.
To Bill Watterson, who inspired me as a kid and still inspires me today.

ACKNOWLEDGEMENTS

PREFACE

"The Land is so much more than its analysis…That man who is more than his elements knows the land that is more than its analysis." –John Steinbeck

TABLE OF CONTENTS

LIST OF TABLES

Table

LIST OF FIGURES

Figure

LIST OF ABBREVIATIONS AND SYMBOLS

β	Ratio of plant to surface drag coefficients
BA	Basal area
BA/FA	Basal-to-frontal area ratio
FA	Frontal area
Γ	Wind shear reduction parameter
h	Sand surface elevation
H_{veg}	Maximum plant height
LLL	Longest leaf length
L_{veg}	Minimum cross-shore distance for vegetation to survive
m	Empirical model fitting parameter accounting for ratio of average to maximum wind shear stress at sand surface
MHW	Mean high water
MSL	Mean sea level
NAVD88	North American Vertical Datum (1988)
ρ_{max}	Maximum vegetative cover fraction
ρ_{veg}	Vegetative cover fraction
σ	Sigma, ratio of plant basal to frontal area
τ	Surface wind shear stress in nonvegetated area
τ_s	Surface wind shear stress in vegetated area
TNC	The Nature Conservancy
t_{veg}	Time for vegetation to reach maximum cover
UTM	Universal Transverse Mercator

ENVIRONMENTAL CONTROLS ON THE GROWTH OF DUNE-BUILDING GRASSES AND THE EFFECT OF PLANT MORPHOLOGY ON COASTAL FOREDUNE FORMATION

1. INTRODUCTION

Barrier islands are low-lying coastal landforms that host valuable and connected ecosystems including salt marshes, maritime forests, and coastal dunes. Barrier islands comprise approximately 15% of the world's coastline (Hayes 1979) and 37 percent of the inhabitants of the United States (more than 100 million people) live in coastal counties (Crowell et al. 2007). In addition, in the U.S., $3 trillion in coastal infrastructure is located on a barrier island coast (Crossett et al. 2004) and coastal tourism generates $373 billion per year (Houston 2008, U.S. Department of Labor 2014). Infrastructure and ecosystems on barrier islands are protected from storm overwash by coastal foredunes, the seaward-most line of coastal dunes (Everard et al. 2010; Barbier et al. 2011).

Coastal foredunes are built from interactions between vegetation and aeolian sediment transport processes (e.g., Hesp 1991; 2002; Keijsers et al. 2015). Grasses tolerant to sand burial facilitate the accumulation of sand moved up the beach face by aeolian transport, leading to formation of a protodune (e.g., Woodhouse 1982; Ehrenfeld 1990; Hesp 2002). The burial tolerant grasses grow as sand accretes (e.g., Ehrenfeld 1990; Gilbert and Ripley 2010), and, if left uninterrupted, a positive feedback between vegetation growth and sand accumulation ultimately builds a foredune populated with mature dune-building grasses (Stallins 2005).

Differences among dune grass species lead to differences in dune morphology (e.g., Woodhouse et al. 1977; Godfrey 1977; Hesp 1989; Hesp 1991; Stallins 2002; Hesp 2004;

1

Hacker et al. 2011). Understanding the effect of different species of dune grass on dune morphology is important because the shape and size of foredunes largely determines how barrier islands respond to climate change-induced shifts in forcing such as sea level rise (Bindoff et al. 2007, Church and White 2006, Pfeffer et al. 2008) and an expected increase in the frequency and intensity of strong tropical storms (Knutson et al. 2013). On the U.S. West coast, variations in plant morphology (growth habit and stem density) have led to variations in dune shape and volume (Hesp 1989; Arens et al. 2001; Hacker et al. 2011; Zarnetske et al. 2012; Seabloom et al. 2013). Along the U.S. mid-Atlantic shoreline, *Ammophila breviligulata* (American beachgrass), *Spartina patens* (Salt meadow cordgrass), and *Uniola paniculata* (Sea oats) (Figure 1), are the primary dune-building vegetation, and the growth forms and geomorphic effects of each grass are different (Woodhouse 1982; Ehrenfeld 1990). Individual plant species influence dune morphology in several ways (e.g.: growth habit (Hesp 1989), stem density (Arens et al. 2001; Hacker et al. 2011; Zarnetske et al. 2012), effective plant height, and the ratio of plant basal-to-frontal area (i.e. the area as viewed from above versus the area viewed from the side of the plant) (Durán et al. 2008).

Much work has focused on plant zonation on coastal dunes—which determines the maximum height to which dunes can grow (Durán and Moore, 2013). Zonation is not encapsulated by a single factor (Barbour and de Jong 1977, Maun 2009), and is thought to depend on two main factors: salt stress (e.g., Oosting and Billings 1942; Wilson and Sykes 1999) and sand burial (e.g., Maun and Perumal 1999; Forey et al. 2008; Maun 2009), though soil water content, wind, nutrients, and pH may also influence plant zonation. The degree and source of these physical stresses (e.g. Oosting and Billings 1942; Martin 1959; Ehrenfeld 1990; Lane et al. 2008; Maun 2009), as well as the community composition (van der Valk 1974; Hayden et al.

1995) and the biological interactions (e.g., Franks 2003; Vick and Young 2011; Young et al. 2011) plants experience can be described by the position each plant occupies as a function of distance to shoreline and elevation. The seaward limit to which dune vegetation can grow has been characterized in Australia (Thom and Hall 1991; Hesp 2013), Brazil (Miot da Silva et al. 2008), and Japan (Kuriyama et al. 2005), and plant growth has been compared across the beach, foredune, interdune, and backbarrier environments in the field (e.g. Oosting and Billings 1942; Woodhouse et al. 1977) and in additional species including forbs and passenger species (e.g. van der Valk 1974; Forey et al. 2008). Even so, field measurements of plant growth rate for the three East coast species of dune-building grass as a function of distance to the shoreline and elevation have not, to my knowledge, previously been made. If environmental stressors, such as those described above, influence where on the backshore a dune grass is likely to grow, this might in turn affect the shape and size of the dune those grasses are able to build.

The ratio of basal-to-frontal area of dune plants is an additional important parameter affecting dune formation, which has not been well studied. Plant basal-to-frontal area determines the degree to which a plant reduces wind speed, thereby reducing surface shear stress. The associated reduction in aeolian sediment transport capacity leads to the local deposition of wind-blown sand and the development of dunes. The ratio of basal to frontal area was measured at approximately 1.5 for desert creosote bushes (Wyatt and Nickling 1997) and Brazilian dune species (Durán et al. 2008), but has not been quantified previously for the dune grasses prevalent on the U.S. East coast.

The purpose of this study was to 1) assess how plant growth (i.e., longest leaf length, basal area, health, and lateral spreading) varies in the field with distance to shoreline and elevation for individual transplants of the three dominant dune-building grasses on the U.S. East

Coast (*A. breviligulata*, *U. paniculata*, and *S. patens)*, and 2) to use frontal and basal area measurements from the field experiment to develop empirically derived parameters for the coastal dune model of Durán and Moore (2013) and perform a suite of model simulations designed to assess how the ratio of frontal-to-basal area—in concert with the other parameters affecting the aerodynamic roughness of a sandy surface—might affect maximum dune height.

2. BACKGROUND

2.1. Field site- Hog Island, VA, Mid-Atlantic Bight

The Virginia Barrier Islands are located on the Eastern Shore of Virginia and comprise the southern stretch of the Delmarva Peninsula. The southern half of this island chain consists of twelve largely undeveloped, mixed-energy barrier islands (Hayes 1979), owned by The Nature Conservancy (TNC), and known as the Virginia Coast Reserve (VCR). Hog Island (located in the middle of the VCR—Figure 2A) is characterized by high topography and dominance of *A. breviligulata* and *S. patens* (Wolner et al. 2013; Dilustro and Day 1997).

The field portion of this study took place on the accretional (Fenster and Dolan 1994) southern end of Hog Island (Figure 2), which provides an ideal location to study *A. breviligulata*, *U. paniculata*, and *S. patens* not only because it is within the naturalized range of each species (Stalter and Lamont 1990; Harvill, Stevens, and Ware 1997), but also because the wide, gently sloping beach and backshore are sparsely vegetated. Here, a foredune approximately 3.5-4 m (NAVD88) high is dominated by *A. breviligulata* and *S. patens* and fronted in places by incipient dunes and protodunes, providing a wide range of combinations of distance to shoreline and elevation within a small geographical area (Figure 2B). TNC approved permits for all parts of this field experiment.

4

2.2. **Coastal Dune Model**

What follows is a brief description of the coastal dune model developed by Durán and Moore (2013), which I will use to explore the effect of frontal-to-basal area on maximum dune height (see Durán and Moore (2013) for more detail). This model simulates the evolution of a sandy, vegetated surface (from the foreshore, across the backshore, and beyond the dune) by calculating aeolian transport and the resultant changes in sand-surface elevation ($\partial h/\partial t$) and vegetation cover fraction ($\partial \rho_{veg}/\partial t$) through time. All model simulations shown in this study were conducted under conditions of a stable foreshore (i.e., the shoreline does not accrete or erode), and a constant onshore wind speed (Table 1).

The coastal dune model captures the two-way interactions between vegetation and sand transport that give rise to coastal foredunes. As the initial model surface evolves, generic 'plants' are able to grow from an initial density of 0 when a given cell is beyond a minimum distance to the shoreline (L_{veg}; the vegetation limit). This generic species has a maximum cover fraction (ρ_{veg}) of 1 and maximum height (H_{veg}) of 1 m, and for simplification, reaches its maximum growth in 3 model days (t_{veg}). Plant growth ($\partial \rho_{veg}/\partial t$) is modified by sand accretion ($\partial h/\partial t$) such that plant growth is maximized when sand accretion is zero, and growth decreases as sand accretion either increases or decreases. Additionally, as vegetation grows ($\partial \rho_{veg}/\partial t$) in a given cell, surface shear stress (τ) is reduced, leading to decreased aeolian sand transport capacity and a growth in the sand surface ($\partial h/\partial t$). The reducing effect of vegetation on wind shear is calculated with the wind shear reduction parameter Γ from Durán and Hermann (2006), based on the work of Raupach et al. (1993):

$$\tau_s = \frac{\tau}{\left(1 + \Gamma \rho_{max}\right)} \qquad (1.1)$$

$$\Gamma = \frac{m\beta}{\sigma} \qquad\qquad (1.2)$$

Where τ_s is the surface wind shear stress in a vegetated area, τ is the surface wind shear in an non-vegetated area, ρ_{max} is the maximum plant cover fraction, β is the ratio of plant to surface drag coefficients, m is an empirical fitting parameter, and σ is the ratio of plant basal area to frontal area. The empirical parameter m takes into account the ratio between average and maximum wind shear stress at the surface across the entire area of interest (Wyatt and Nickling 1997). Durán and Moore (2013) parameterize (1.1) and (1.2) based on previous work on desert creosote shrubs. It is these parameterizations that will be replaced below with empirically derived measurements of plant basal and frontal area.

3. METHODS

3.1. **Experimental setup**

On May 21, 2014, I planted 2 individuals of each species at 30 locations in each of two ~25 m wide cross-shore swaths on the southern end of Hog Island (Figure 2B) (for a total of 360 plants at 180 locations). Using transplants that had been grown from seed in greenhouses, I first sorted seedlings by length and number of stems and then selected the intermediate-sized seedlings for planting to reduce initial variation among individuals. To further reduce variation, I trimmed (before planting) the leaves of *A. breviligulata* and *U. paniculata* seedlings to 25 cm and those of *S. patens* to 20 cm, as not all *S. patens* seedlings had leaves longer than 20 cm. I installed additional plants in a reserve garden at the base of the dune south of the southern transect. Plant locations were marked with fiberglass stakes and labeled according to species, swath, and distance from the shoreline (i.e., the mean high water line; MHWL). I installed plants at any given location approximately 5 cm away from the fiberglass stake, 10 cm away from one another, and 2 cm below the sand surface and coded each plant according to its location.

To minimize the effect of plant mortality due to transplant shock on my results I replaced dead plants with live ones from the reserve garden (which was cared for in the same way as the experimental plantings) until June 23. Upon initial and replacement planting, I applied 300 mL of fresh water at the base of the plant. I applied an additional 120 mL of fresh water to each plant on May 21, 22, 23, and 29, and June 5, 9, 13, and 23. To reduce competition with pre-existing vegetation, I removed (monthly) the aboveground biomass of pre-existing vegetation within 1 meter of each plant location, measured from the fiberglass stake. On June 24, I removed the aboveground biomass of the plant with fewer or weaker leaves at each location to reduce competition between adjacent transplants. If the removed plant grew back, its aboveground biomass was removed monthly.

Based on data collected at a meteorological station on Hog Island (Porter et al. 2014a) the summer of 2014 was wetter than average (Figure 2A-B), and thus the transplants in this experiment received more precipitation than would be expected in a normal summer in this location. Rainfall events delivering in excess of 20 cm of rain were more frequent in 2014, especially in July, than in the two years previous (Figure 3A), and precipitation in September was greater than 1 standard deviation higher than the September mean computed over the last 25 years (Figure 3C). Wind predominantly blew onshore over the field season, with dominant modes from the south and from the southeast (Figure 3C).

Two noteworthy meteorological events occurred at the experimental site during the 2014 experimental season. First, the eye of Hurricane Arthur passed 150 km to the south of the site on July 4, 2014, bringing winds of 11.5 m/s to Hog Island (Porter et al. 2014a). Second, an intense rainfall event occurring from September 7 to September 9 (138.38 mm of rain over the 3 days, Porter et al. 2014a) delivered one-third of all the rainfall throughout the entire field season (May

21 to October 14) (Figure 3A) and combined with an astronomical spring high tide on September 10 to generate one of the highest high water events observed throughout the field season.

Plant locations varied from 21.3 m to 103.5 m in distance to the shoreline, and from 1.25 to 3.78 m in initial elevation. The locations highest in elevation were on the foredune ridge, whereas those lowest in elevation were at the foredune toe and the seaward edge of transect A (the southernmost swath). To cover a wide gradient of distance to shoreline and elevation, I installed transplants across two protodunes located in the northern swath at approximately 50 to 70 m and 80 to 85 m from the shoreline, having maximum elevations of 2.4 and 2.5 m, respectively, and on a single, smaller protodune (maximum elevation of 2.0 m) in the southern swath between 40 and 50 m from the shoreline (Figure 2B).

3.2. **Measurements**

I made a series of measurements and observations (longest leaf, plant state and elevation) monthly from June to October in 2014. I measured longest visible leaf length to the nearest millimeter with a repeatability of +/- 1 mm between observers, and this is the measurement used in allometric relationships. In cases where the sand surface at a plant location eroded, I measured the longest visible leaf from the base of the plant – not the sand surface around the transplant soil plug. I calculated longest leaf length—the measure of plant growth used in regression analyses— by subtracting the initial elevation from the October elevation at each plant site and then adding that value (if it was positive) to the measurement of longest visible leaf collected in the field to account for accretion at each plant site.

Each month, I measured plant mortality, or "plant state," by visually observing the color, uprightness, and number of plant leaves, as well as the presence or absence of each plant. I

classified plants as "Healthy," "Stressed," "Dead," or "Missing," and I collected photographs of each plant for additional evidence of plant state (Figures S1-S3, Appendix 3).

To measure elevation, I installed two GPS monuments on the secondary dune ridge at the experimental site, collected the UTM coordinate and NAVD88 elevation of one using a Trimble R6, and post-processed the point using the National Geodetic Survey's Online Positioning User Service (NGS-OPUS) (XY error = 0.008 m, Z error = 0.022 m). I then used a Nikon DTM-322 total station to measure the elevation of the second monument (angle error = 5 arcseconds), and confirmed its position with a later GPS survey according the procedure described above. I then used the total station and backsight to survey the elevation at the fiberglass stake at each plant location, as well as in the reserve garden. I also collected four monthly cross-shore beach profiles along repeated transect lines (one through each experimental swath, and one each to the north and the south of the two swaths) from the primary foredune to the water line by collecting a point at each change in slope along the profile (Figure 4). To measure distance to the shoreline, I calculated the NAVD88 elevation of mean high water (MHW) at the experimental site (0.46 m NAVD88) using VDATUM (NOAA). Using ArcGIS, I then created a shore-parallel line at this elevation in the June topographic survey and measured the shortest shore-perpendicular distance from that line to each plant location. I made additional measurements (lateral spreading, basal area, and frontal area) at the beginning and/or end of the field season. Similar to plant mortality, I measured lateral spreading visually as a binary variable (spreading vs. no spreading). Given that each species has a different growth habit and rate of lateral spreading I identified lateral spreading in *A. breviligulata* and *S. patens* if rhizomes were visibly growing from below the ground surface away from the main plant. I identified spreading in *U. paniculata* when I observed multiple clusters of spreading centers, each with its own radial symmetry, at a plant

9

(Figure S4). To measure the basal and frontal area of each plant, I photographed each plant in the

plan (basal) and front (frontal) view in June and October, then used the ImageJ software package

to calculate the plant area in square centimeters (Figure S5).

I made two measurements on September 10 that were only possible due to the high water

event on that day. First, I measured the salinity of a water sample from a pool of standing water

near the foredune toe, and second, I surveyed the elevation of a wet/dry line on the foredune and

protodunes, then calculated the average elevation of these points.

For more details on methods, please see Appendix 1.

3.3. **Data Analysis**

I created interpolated surfaces in ArcGIS based on the monthly elevation surveys, then

used the Minus function in ArcGIS to subtract the June surface from the October surface. This

created a topographic change map for the growing season (Figure 5).

To compare the continuous transplant growth parameter, longest leaf length in living

plants, with continuous environmental parameters (including distance from the shoreline, initial

elevation, and change in elevation), I used 2-parameter and multiparameter linear regression as

well as 2-parameter quadratic regression (for change in elevation). I then derived an optimized

multi-parameter equation (based on maximizing the number of significant coefficients and the

adjusted R^2 value while minimizing the number of non-significant coefficients) for each species

relating longest leaf length to the environmental parameters. I used nonlinear regression to

analyze the relationships between basal area and initial elevation. Additionally, postdoctoral

associate Dr. Evan B. Goldstein assisted me by using nonlinear regression following the

approach of Schmidt and Lipson (2009) to calculate equations relating longest leaf length and

frontal or basal area.

I calculated total water level using data from a tide gauge on the north side of Hog Island (Porter et al. 2014b) and a wave buoy offshore of Cape Henry, VA (NOAA/Scripps Institution of Oceanography Waverider Buoy #44099, 36°54'55" N, 75°43'12" W). I then compared the TWL record to plant mortality (Figure 6A), calculated as a percentage: the number of missing or dead plants within a 0.1-m bin observed in a given month divided by the total number of plants present in the previous month.

The high water event of September 10 resulted in pools of standing water at low elevations for at least one day. The tide was the highest of the field season on this day (Porter et al. 2014b), but the total water level (TWL, defined as the measured water elevation plus the elevation of runup of the highest 2% of waves, Ruggiero et al. 2001) at the experimental site was higher on October 4. But, since I was able to make measurements at the field site on September 10, to capture the impacts of a high water event on topography and plant growth, and to measure the salinity of surface water near the dune, I focus below on the event of September 10th.

Because increases in ocean water level driven by the tide are known to drive increases in the elevation of the freshwater lens underlying a barrier island (e.g., Philip 1973, Smiles and Stokes 1976, Urish and McKenna 2004), I performed a series of analyses to assess plant growth in low areas where access to water substantially increased in comparison to relatively higher areas where access to water increased less. The maximum total water level during the field season was 1.8 m on October 4, so using this level as a proxy for water access, I created three elevation classes (low, high and middle) within the transplanted range: 1) plants below the maximum total water level for the field season (elevation < 1.80 m), 2) plants above the average elevation of the wet/dry line observed and surveyed on September 10 (elevation > 2.02 m), and 3) plants located at elevations between 1.80 m and 2.02 m (Figure 7). I compared plant growth as

measured at the end of the growing season in October by basal area, plant health, and lateral spreading across all species and all three elevation zones.

For these categorical plant growth and elevation analyses, I compared log basal area to elevation classes using 1-way ANOVA; and compared plant health and lateral spreading to elevation classes using a Chi-squared test. I performed a log transformation on basal area values before analysis to give the data a more normal distribution and enable the use of ANOVA instead of a less statistically powerful non-parametric test (e.g. Kruskal-Wallis) (Figure 10A inset).

Model runs in this study followed the parameterization of Durán and Moore (2013), with the addition of a Heaviside function in the vegetation dynamics equation describing a minimum elevation above mean sea level (MSL) for vegetation growth (z_{min}, Durán and Moore 2014) (Table 1). I varied the ratio of basal-to-frontal area (σ) across values ranging from 0.1 to 2.0, and varied the empirical fitting parameter m over the range 0.1 to 0.2, incorporating the values suggested by Wyatt and Nickling (1997).

4. RESULTS

4.1. Topographic change

Comparison of topographic profiles collected at the beginning and the end of the field season indicates areas of vertical accretion and areas of erosion, with topographic changes ranging from +1.0 to -0.3 m (Figures 4 and 5). Sediment accumulated (0.1 – 1.0 m) at the seaward end of each transect, likely due to onshore transport of sand from the nearshore during the summer season. Sediment also accumulated at the seaward edge of the foredune (0.1 – 0.56 m), likely due to aeolian accretion. Erosion occurred primarily in areas of initially high elevation (on top of the foredune and on top of the protodunes; 0.1 – 0.3 m) (Figure 5). A channel, which cut through the northern swath during the high water event on September 10 (Figure 4B),

temporarily lowered the topography by 0.2 m at a distance of approximately 150 m from the June shoreline along this transect.

4.2. **Growth relationships**

In the 2014 growing season, *A. breviligulata* transplants grew to a maximum longest leaf length of 928 mm and maximum basal area of 2402 cm^2. For *S. patens*, these values were 792 mm and 1018 cm^2, and for *U. paniculata*, they were 1185 mm and 2869 cm^2.

In *A. breviligulata*, longest leaf length was significantly correlated with change in elevation through a quadratic equation, and in *S. patens* and *U. paniculata*, longest leaf length was significantly correlated with all three environmental parameters (distance to shoreline, initial elevation, and change in elevation) through a multiparameter linear equation (Tables 2 and S1; $p<0.01$, $p=0.01$, $p<0.01$; Adjusted $R^2=0.38$, 0.18, 0.43; respectively). In *A. breviligulata*, longest leaf tended to increase with change in elevation up to 0.13 +0.35/-0.08 m of change, after which longest leaf tended to decrease (Figure 8D). Increases in change in elevation and decreases in distance to shoreline and initial elevation were correlated with increases in longest leaf length in *S. patens* (Table 2), and these relationships held at a higher level of significance but equal level of predictive power when distance to shoreline and initial elevation were analyzed separately from one another (Table S1, Appendix 2). In *U. paniculata*, increases in distance to shoreline and change in elevation and decreases in initial elevation were significantly correlated with longest leaf length (Table 2).

If change in elevation is excluded, distance to shoreline and elevation had no significant relationship with longest leaf length for any species either alone (Figure S6) or together in a multiple linear equation (Table S2). Additionally, longest leaf length in *A. breviligulata* was not significantly correlated with distance to shoreline or elevation in any regression (Figure S6). ,

Tables S2-S4). Longest leaf length had a significant, positive, simple linear correlation with change in elevation in *A. breviligulata* and in *U. paniculata*, but not in *S. patens* (Figure 8A-C; $p<0.01$, $p=0.11$, $p<0.01$; $R^2=0.28$, 0.05, 0.34; respectively). Quadratic regression yielded a significant relationship between longest leaf length and change in elevation in *A. breviligulata* only (Figure 8D-F).

Large differences in the magnitudes of the coefficients in these relationships arise from differences in the ranges of each environmental parameter (~20–120 m for distance to shore; ~1–4 m for initial elevation; ~ -0.2 – +0.3 m for change in elevation), and when these coefficients are rescaled to units on the same order of magnitude, regression results (p, t, F statistics) do not change. Belsley's test for collinearity returned collinearity indices less than 11 for all combinations of independent variables in all species – far lower than the threshold level of 30 – indicating that multicollinearity did not significantly affect my results. Additionally, sample size was large enough (N>>15) for all relationships to be robust to modest violations of normality, though probability plots of residuals showed no such violations.

Plant mortality qualitatively tended to be observed after high water events (Figure 6A) and at the edges of swaths, dunes, and protodunes (Figure 6B).

4.3. **Plant Growth and Access to Water**

In general, living plants of all species at low initial elevations (e.g., between ~1.2 m and ~1.75 m; near the shoreline and near the dune toe) tended to grow larger (basal area) than plants across a broader range of higher elevations (i.e., ~2.0 m to ~4 m) (Figure 9). The dense cluster of plants at low initial elevations and small basal areas with two longer tails along the x- and y-axes suggests that basal area is a more continuous (rather than discrete) function of elevation (Figure 9B). Most data tend to appear in the low-basal area and low-elevation zone, between

14

~1.5 m and ~1.75 m. Nonlinear regression on the basal area vs. initial elevation data produces a fitted power-law equation (RMSE=387, lower for *A. breviligulata* and *S. patens*), and qualitatively shows the nature of the relationship between basal area and initial elevation (Figures 9A, S7). These power-law equations are descriptive of my data and should not be interpreted as describing a physical process due to the large exponential terms ($\sim x^8$).

The salinity of the standing water near the foredune toe on September 10th was 0.15 ppt, indicating a freshwater source. Living plants in the low zone had significantly larger log-transformed basal areas than those in the mid zone or high zone. (340 vs. 95 and 107 cm^2, respectively, 1-way ANOVA, p<0.01) (Figure 10A). A Kruskal-Wallis test on the untransformed data yielded qualitatively the same result as the ANOVA test on the log-transformed data, and p-values for both were orders of magnitude lower than 0.01. These relationships hold when normalizing each individual measurement by dividing the longest leaf lengths and basal areas of each plant by the maximum of each species. Plants were not significantly healthier in any zone compared to the others (Chi-square, p=0.47; Figure 10B), but healthy plants in the low zone were significantly more likely to spread laterally than those in the mid or high zones (Chi-square, p<0.01; Figure 10C).

There were no significant differences among species in normalized log basal area, plant health, or lateral spreading that held across all zones, though small sample size may have contributed to these results (Table 3), though of the three species, *S. patens* was the most likely to spread laterally in the low zone, while *A. breviligulata* was the least likely to spread laterally in the low zone.

4.4. **Plant Basal vs. Frontal Area**

My field data provides quantitative constraints on the ratio of basal-to-frontal area (σ, Durán and Hermann 2006, Durán et al. 2008, Durán and Moore 2013) most appropriate for dune-building grasses. All dune grasses in this experiment had $\sigma = 0.8$ +/- 0.3 (mean +/- 1 S.D.), which differs significantly from the mean value of ~1.5 reported for creosote bushes (Wyatt and Nickling 1997) and Brazilian dune plants (Durán et al. 2008) (Figure 11A).

Basal and frontal area measurements are difficult and time-consuming to make, both in the field and in post-processing. However, longest visible leaf measurements are simple, quick, and require no post-processing. For this reason, I investigated the relationship between longest leaf length and plant size, and I derived allometric relationships for basal and frontal area as a function of longest visible leaf length, which take the form $y=Ax^b$ (where y is the basal or frontal area, x is the longest visible leaf length, and A and b are coefficients) (Figure 12, Table 4).

In the coastal dune model of Durán and Moore (2013), an increase in the ratio of basal to frontal area acts to amplify the reducing effect of vegetation on surface wind shear and thereby reduce the wind shear near a plant (Equations 1 and 2). Results from this model showed that changes in the ratio of basal area to frontal area had a nonlinear effect on maximum dune height (Figure 11B). As the ratio increased (greater basal area proportional to frontal area), dune height increased until the ratio reached ~0.85, then decreases sharply when the ratio is equal to 1.3. At ratios greater than 1.3, dune height tended to decrease gradually. This nonlinearity arose from the mathematical relationship between wind shear stress and vegetation (Equations 1 and 2). The ratio of basal-to-frontal areas did not vary significantly among the species in this study; therefore modeled maximum dune height in my experiment was not controlled by species-specific variations in plant morphology.

Varying the empirical fitting parameter m changes the BA/FA value at which the nonlinear transition occurs (Figures 11, S8). Within the range suggested by Wyatt and Nickling (1997), m has a small effect on maximum dune height, but the effect of m increases as the ratio of basal-to-frontal area increases. The m parameter also acts to change the BA/FA value at which the nonlinear transition occurs- when m equals 0.1, the nonlinear transition in dune height occurs around a BA/FA value of 0.9 (instead of 1.3), and an increase in m by 0.02 units causes the center of the nonlinearity to increase by 0.2 BA/FA units.

5. DISCUSSION

5.1. Growth relationships

Multiparameter regression suggests significant species-specific correlations between growth (as measured by longest leaf length) and distance to shoreline, elevation, and change in elevation that were not apparent from simple regression analyses (Table 2, Figure S6). For *A. breviligulata* and *U. paniculata*, these environmental parameters accounted for a fairly large portion of the variance in growth among individuals (Adj. $R^2 = 0.38$ and 0.43 respectively), but these parameters were not as strong of a predictor of growth in *S. patens* (Adj. $R^2 = 0.18$). The ability of *S. patens* to occupy a wider range of environments (Anderson and Alexander 1985; Craig 1975; Stalter et al. 1999) than *A. breviligulata* or *U. paniculata* may explain the relative lack of predictive strength in the correlation between the longest leaf length of *S. patens* and environmental conditions across the dune and beach.

For *A. breviligulata*, change in elevation was the only environmental parameter significantly correlated with longest leaf length, and quadratic regression suggested a maximum in longest leaf length at 0.13 +0.35/-0.08 m of sand accretion (Figure 8). In *S. patens*, no single parameter was significantly correlated with longest leaf length (Figure S6), though when change

in elevation was taken into account, longest leaf length was significantly positively correlated with change in elevation and negatively correlated with initial elevation and distance to the shoreline (Tables 2 and S1). When change in elevation, distance to the shoreline, and initial elevation were considered together, only change in elevation was significantly correlated with longest leaf length (Table 2). When considering each parameter individually for *U. paniculata*, longest leaf length was significantly positively correlated only with change in elevation (Figure 8). However, when all factors were considered together, longest leaf length was significantly positively correlated with distance to the shoreline and change in elevation, and significantly negatively correlated with initial elevation (Table 2). These results are summarized in Table 5.

The tendency for salt spray and soil salinity to decrease with increasing distance from the shoreline and the increased ability of *S. patens* over *U. paniculata* to cope with salinity stress (Seneca 1972) may account for the difference in sign of the correlation for these two species. The negative correlation between longest leaf length and initial elevation (i.e., faster growth at low elevations) observed in both species may be due to increased availability of water at low elevations (Section 5.2).

The significant positive correlation between plant growth and change in elevation across all three species is consistent with previous evidence suggesting that sand accretion is the primary driver of dune plant growth and zonation (Maun and Perumal 1999; Forey et al. 2008; Maun 2009). Because changes in dune surface elevation are wind-driven, local wind conditions may play a role in determining total plant growth observed at a given site with a given time. For example, if the local winds had been more consistently onshore (versus as in Figure 3C) during our experiment, more sand may have been transported from the beach into the vegetated area, therefore leading to more plant growth overall, given the observed positive correlation between

sand accretion and plant growth across species. That plant growth and change in elevation are positively correlated (i.e., faster growth is associated with accretion/burial) for individuals of *U. paniculata* provides quantitative evidence in further support of its classification as an effective "dune-builder" (e.g., Woodhouse 1982; Ehrenfeld 1990; Stallins 2002; Stallins 2005), and the same is true for *A. breviligulata* up the rate of change in elevation that maximizes plant growth (i.e., 0.13 +0.35/-0.08 m over 5 months). Additionally, the less positive correlation in *S. patens* between the same two factors agrees with literature (Travis 1977; Stallins 2005; Wolner et al. 2013; Brantley et al. 2014) characterizing *S. patens* as a grass tolerant of, but not as responsive to, sand accretion as other dune-building species. The quadratic relationship I derived for *A. breviligulata* is similar to that derived by Maun and Perumal (1999) relating sand burial to cover of *A. breviligulata*. When the data points with the four most extreme Δz values were removed from the *A. breviligulata* data, the quadratic equation no longer significantly fit the data, but change in elevation was still the only environmental factor significantly correlated with longest leaf length (Table S5).

Continuing work with this dataset and data from the same plants over a second growing season will further investigate the relationship between sand accretion, plant growth, and aerodynamic roughness, especially to relate plant growth measured in the field to plant growth in the Durán and Moore (2013) model. The results of this experiment suggest that species-specific growth patterns could be approximated in the coastal dune model by including a factor that incorporates sensitivity to distance to the shoreline in the vegetation growth equation. For example, for a model species representing *U. paniculata* (*S. patens*), a multiplier could be included in the equation for growth rate to reflect an increase (decrease) in the rate of growth with increasing distance to the shoreline. For a species representing *A. breviligulata*, this

multiplier could be set to unity, as growth in *A. breviligulata* was not significantly correlated with distance to the shoreline.

Though plant growth was significantly correlated with distance to shoreline, initial elevation, and change in elevation, controls on mortality and the associated cross-shore vegetation limit (i.e., L_{veg}, Durán and Moore 2013) were not apparent in data arising from the first growing season of this field experiment (Figure 6B). If the seaward limit beyond which dune-building vegetation does not successfully grow arises from plant responses to stresses associated with beach position (e.g., salt spray, sand burial, wind, etc.), it may be that it will take longer than one growing season for these stresses to cause mortality in my transplants. Alternatively, if this limit is controlled by responses to physical processes associated with storms—such as high total water levels and an elevated zone of wave action—it is possible that the plants in my experiment, which were artificially planted near the shoreline as fairly substantial individuals, may have persisted through the first field season because a HWE sufficiently large to damage or physically remove them had not yet occurred. The idea that physical processes (e.g. salinity stress, mechanical erosion) associated with storms may control the seaward limit of growth is consistent with my observation that TWL was relatively low compared to the elevation of most of the plants throughout the growing season, but that after high water events such as Hurricane Arthur and the September 10th HWE, I tended to observe plants to be dead or missing at elevations below the total water level associated with these events (Figure 6A). Similar observations have been made in a natural dune system in the Netherlands (de Winter et al. 2015; van Enckevort and Ruessink 2001), where dune grasses growing seaward of the dune crest were washed out periodically. Additionally, Kuriyama et al. (2005) observed

20

vegetation establishing seaward of the dune crest up to the extreme limit of runup, further suggesting a link between TWL and vegetation zonation.

Additionally, it is possible that individual plant survival during storms depends on plants becoming established, accreting sand, and potentially binding this sand with their roots against wave action (as occurs in fluvial and riparian systems (e.g., Gurnell et al. 2001, Tabacchi et al. 2000) between high water events. In my experiment, two plants (marked in Figure 6B) were established and growing before they were killed and removed during HWEs. The older, denser preexisting vegetation at similar distances from shoreline and elevations, which presumably had a larger, denser root system than did the transplants, survived the same high water events. It is possible that with the increased stabilization afforded by large root systems, these plants would have survived the high water events had they occurred after the plant had become more established.

In addition to the potential importance of individual plant characteristics in determining whether or not a plant will survive during a HWE, it is possible that survival during a high water event depends on emergent properties of the plant community. For example, many of the plants that died and/or were removed during my experiment were near the edge of a swath or protodune (Figure 6B). Thus, these plants were not surrounded by others in the community and may have been subject to higher wave and salinity stresses from the high water event relative to plants having a more interior location. Perhaps in a densely populated area, edge plants block salt spray, attenuate wave action, as in the salt marsh environment (e.g., Kobayashi et al.1993; Borsje et al. 2011; Möller et al. 2014), or enable greater sand accumulation due to increased stem density (Hacker et al. 2011) in the more densely populated area, increasing the likelihood that interior plants will survive.

21

Decreased survival along the edges of swaths and protodunes, along with qualitatively high rates of growth and topographic change in the reserve garden (personal observations), points to a potential facilitative relationship among dune grass individuals (which we are preparing to explore in future experiments) promoting growth, survival, and density, as suggested by Castanho and colleagues (2015). This idea is in agreement with the Stress Gradient Hypothesis (e.g. Bertness and Callaway 1994; He et al. 2013), which predicts that high levels of stress will lead to increased facilitative relationships among individuals.

5.2. **Plant Growth and Presence of Water**

Longest leaf length and initial elevation had a significant negative correlation in *S. patens* and *U. paniculata* (Tables 2 and S1), and in general, transplants of all species installed at low elevations had larger basal areas and were more likely to spread than those at higher elevations (p<0.01, Figure 10).

Due to the observed patterns of plant growth, I believe that in addition to change in elevation, access to water is important in determining plant growth, especially for transplants, which have shallow root systems and therefore cannot access groundwater when planted at higher elevations. The low salinity in the water sample collected from the isolated pool of surface water on the backshore following the coincident rain event of September 7-9 and the HWE of September 10, suggests that in low areas following rainstorms and/or HWEs, accumulations of fresh water and/or groundwater pumped upward from the freshwater lens during the tidal cycle may provide access to water for plants at low elevations, potentially allowing them to grow more than the transplants at higher elevations. Though this appears to conflict with previous findings in *U. paniculata* (Oosting and Billings 1942; Hester and Mendelssohn 1989) and *S. patens* (Naidoo et al. 1992; Burdick 1989; Burdick and Mendelssohn

1987), none of these studies investigated plant growth along a continuum of elevation in the field. Future work will investigate the elevation and salinity of the water table at the experimental site and provide more insight into the groundwater hypothesis.

It follows that transplants installed at relatively high elevations (as they are in dune restoration projects) would benefit from having long root systems at the time of installation so that they are able to reach the groundwater table as consistently as transplants installed at relatively lower elevations, or from being installed at a lower initial elevation (consistent with Nordstrom et al. 2000, Nordstrom 2008). In naturally evolving systems, such elevation-related sensitivity to water is likely diminished because grasses grow upward as the sand surface accretes (e.g. Ehrenfeld 1990, Gilbert and Ripley 2010), leading to the development of deep roots which extend deep into the subsurface, likely to the base of the dune.

5.3. **Plant Basal and Frontal Area**

The ratio of basal-to-frontal area of the transplants in my field experiment is close to the value that maximizes dune height in the coastal dune model of Durán and Moore (2013) when the *m* parameter is equal to 0.16 (as in Durán and Moore 2013; 2014). Several studies correlate dune morphology to vegetation morphology (Hesp 2002, Hacker et al. 2011, Zarnetske et al. 2012, Seabloom et al. 2013) and model results presented here—which show that the ratio of plant basal-to-frontal area exerts a nonlinear control on maximum dune height—suggest that the model is capturing this dependence. All other factors being equal (e.g., sand supply, wind direction and velocity, tidal range, etc.), dunes built by the grass species of interest in this experiment (*A. breviligulata*, *S. patens*, *U. paniculata*) and other grasses of similar shape (BA/FA = 0.8) will be taller than those built by grasses of a shape more similar to those previously studied (BA/FA=1.5, Wyatt and Nickling 1997; Durán et al. 2008) (Figures 11, S3).

This suggests that measuring the basal and frontal area for different dune grass species may be important in predicting the maximum dune height that can naturally be achieved in a given location and the protection from overwash and inundation that may be afforded by dunes built by different grass species.

It is possible that the lower ratios of basal-to-frontal area observed in my experiment were due to individual transplants being installed with ample space to spread out in the lateral dimensions to absorb light. In a naturally spreading dune system in which plants are spreading clonally, individual plants are packed densely together, and plants are thereby forced to grow more vertically than horizontally to absorb light, and this could have lead to an artificially decreased ratio of basal-to-frontal area in my experiment (future experiments will compare the ratios of basal-to-frontal area of transplants to plants naturally growing in the experimental site).

Since basal and frontal area are important parameters controlling dune height, it is useful that longest visible leaf length predicts basal and frontal area through an allometric scaling relationship for each species (Table 4). Basal and frontal area are difficult and time-consuming measurements, both in the field collection stage and in the image processing stage, but longest visible leaf length is a very simple and quick field measurement that requires no further processing.

6. CONCLUSIONS

Transplant longest leaf length was most significantly correlated with change in elevation in all species, and growth was also correlated with distance to shoreline and initial elevation in *S. patens* and *U. paniculata*. Quadratic regression suggested a maximum in plant growth of *A. breviligulata* at an accretion rate of ~0.1 m over one growing season. Distance to shoreline was oppositely correlated with growth in *S. patens* (negative correlation) and *U. paniculata*

(positive), possibly due to differences in salinity tolerance in each species. Longest leaf length and initial elevation had a significant negative correlation in *S. patens* and *U. paniculata*, and transplants of all species were largest and most likely to spread at low elevations, and I attribute this to increased access to water. Future modeling work will investigate species-specific effects on foredune morphology in response to environmental parameters.

Additionally, longest visible leaf length scales allometrically with basal and frontal area across species, enabling the use of a simple measurement to approximate aerodynamic roughness parameters. Though the ratios of basal to frontal area are different for the U.S. East coast dune grasses (0.8) than for plants studied previously (1.5), they do not vary significantly among the East coast species, and this ratio exerts a nonlinear control on maximum foredune height predicted by the Durán and Moore (2013) coastal dune model. Simulations suggest that, other factors being equal, foredunes are highest at a ratio of basal-to-frontal area of ~0.8, which is the ratio measured for the East coast dune-building grasses.

From my results, I extrapolate that restoration projects working to optimize environmental conditions specific to each species will be the most successful. Projects could benefit from installing transplants of *S. patens* closer to the shoreline than those of *U. paniculata*, and projects involving all species would benefit from maximizing plant access to water while promoting a moderate amount of sand accretion and maintaining dune structure.

TABLES

Parameter Name	Description	Value Used	Reference
NX	Cross-shore cells	100	Durán and Moore (2013)
NY	Shore-parallel cells	4	Durán and Moore (2013)
Nt	# of Timesteps	100,000	Provides ample time for model to reach maximum height
u	Shear velocity (m/s)	0.35	Durán and Moore (2013)
L_{veg}	Cross-shore vegetation limit (m)	15	Durán and Moore (2013)
z_{min}	Vertical vegetation limit (m)	0.1	Durán and Moore (2014)
t_{veg}	Time for vegetation to fill cell (d)	3	Durán and Moore (2013)
σ	Plant ratio of basal-to-frontal area	*varied*	Varied from 0.1 to 2.0 to incorporate field measurements (σ=0.8) and values suggested by Wyatt and Nickling (1997) and Durán et al. (2008) (σ=1.5).
β	Ratio of drag coefficients of plant to bare sand	150	Raupach et al. (1993), Wyatt and Nickling (1997), Durán and Moore (2013)
m	Empirical shear reduction parameter	*varied*	Varied every 0.02 units from 0.10 to 0.20 to incorporate the suggested range of 0.14 to 0.18 suggested by Wyatt and Nickling (1997)

Table 1. Parameter list. List of parameters used in the modeling portion of this experiment and their respective values, units, and sources.

A. breviligulata $LLL = A + B\Delta z + C\Delta z^2$			
Coefficient	**Value**	**95% CI (+/-)**	**t-statistic**
A**	640	35	37
B**	1500	540	5.6
C**	-5900	3800	-3.1
N= 50, DOF= 47, RMSE= 105, R^2= 0.40, Adj. R^2= 0.38 F-statistic vs. constant model: 16, $p < 0.01$			

S. patens $LLL = A + Bz + Cx + D\Delta z$			
Coefficient	**Value**	**95% CI (+/-)**	**t-statistic**
A**	660	130	9.9
B	-41	76	-1.1
C	-1.8	2.0	-1.9
D**	900	620	2.9
N= 48, DOF= 44, RMSE= 113, R^2= 0.23, Adj. R^2= 0.18 F-statistic vs. constant model: 4.4, $p = 0.01$			

U. paniculata $LLL = A + Bz + Cx + D\Delta z$			
Coefficient	**Value**	**95% CI (+/-)**	**t-statistic**
A**	640	190	6.8
B**	-138	93	-3.0
C*	3.4	2.8	2.4
D**	1900	710	5.5
N= 45, DOF= 41, RMSE= 162, R^2= 0.47, Adj. R^2= 0.43 F-statistic vs. constant model: 12, $p < 0.01$			

Table 2. Results of multiparameter regression. Optimized multiparameter equations (based on combination of significant coefficients and adjusted R^2 values) relating longest leaf length (mm) to distance to shoreline, initial elevation, and change in elevation (m) in each species. Coefficients, 95% confidence intervals, and the t-statistic for each variable are shown, with p values <0.05 marked with * and p values <0.01 marked with **. Goodness-of-fit statistics (Number of replicates (N), Degrees of freedom (DOF), Root mean square error (RMSE), R^2, Adjusted R^2) and the F-statistic and p-value for the overall fit equation at bottom.

		Low			Middle			High		
	Plant	**NM**	**SE**	**p-val**	**NM**	**SE**	**p-val**	**NM**	**SE**	**p-val**
Basal Area	*A.b.*	0.32	0.05		0.10	0.04		0.08	0.02	
	S.p.	0.32	0.05	0.49	0.04	0.03	0.38	0.06	0.02	0.44
	U.p.	0.24	0.05		0.10	0.04		0.09	0.02	
log Basal Area	**Plant**	**NM**	**SE**	**p-val**	**NM**	**SE**	**p-val**	**NM**	**SE**	**p-val**
	A.b.	0.81	0.03		0.70	0.06		0.64	0.03	
	S.p.	0.78	0.03	0.14	0.51*	0.04*	0.05*	0.57	0.03	0.18
	U.p.	0.74	0.03		0.66	0.05		0.63	0.03	
Plant Health	**Plant**	**H**	**U**	**p-val**	**H**	**U**	**p-val**	**H**	**U**	**p-val**
	A.b.	30	4		3	3		15	5	
	S.p.	26	8	0.28	5	1	0.47	14	6	0.77
	U.p.	25	9		4	2		16	4	
Lateral Spreading	**Plant**	**S**	**N**	**p-val**	**S**	**N**	**p-val**	**S**	**N**	**p-val**
	A.b.	9	21		0	3		1	14	
	S.p.	18*	8*	0.01*	1	4	0.66	4	10	0.28
	U.p.	12	13		1	3		4	12	

Table 3. Species comparison within elevation zones. Comparisons among species within three elevation zones. Significant differences (p<0.05) among species within a zone are marked with *. "NM" is the normalized mean (mean of data normalized to the maximum value for each species), "SE" is the standard error, "H" is the number of healthy plants in that species and zone, "U" is the number of unhealthy plants in that species and zone, "S" is the number of plants that spread laterally in that species and zone, and "N" is the number of species that did not spread laterally in that species and zone.

	A. breviligulata	*S. patens*	*U. paniculata*
Basal Area	$(1.53 \times 10^{-8}) * LvLL^{3.73}$	$(8.13 \times 10^{-9}) * LvLL^{3.85}$	$(2.26 \times 10^{-9}) * LvLL^{3.94}$
	RMSE=325	RMSE=130	RMSE=308
Frontal Area	$(1.55 \times 10^{-8}) * LvLL^{3.77}$	$(1.30 \times 10^{-8}) * LvLL^{3.84}$	$(2.94 \times 10^{-9}) * LvLL^{3.93}$
	RMSE=370	RMSE=248	RMSE=420

Table 4. Longest visible leaf length vs. Basal and Frontal Areas. Allometric relationships

between longest visible leaf length and basal and frontal area, with root mean square error.

Environmental parameter	*A. breviligulata*	*S. patens*	*U. paniculata*
Change in elevation	++	+	++
Distance to shoreline	**x**	-	+
Initial elevation	**x**	-	-
Adjusted R^2	0.38	0.18	0.43

Table 5. Summary of multiparameter regression. Summary of the results of multiparameter regression. "+" indicates positive correlation with longest leaf length, "++" indicates more significant positive correlation, "-" indicates negative correlation, and "x" indicates no significant correlation.
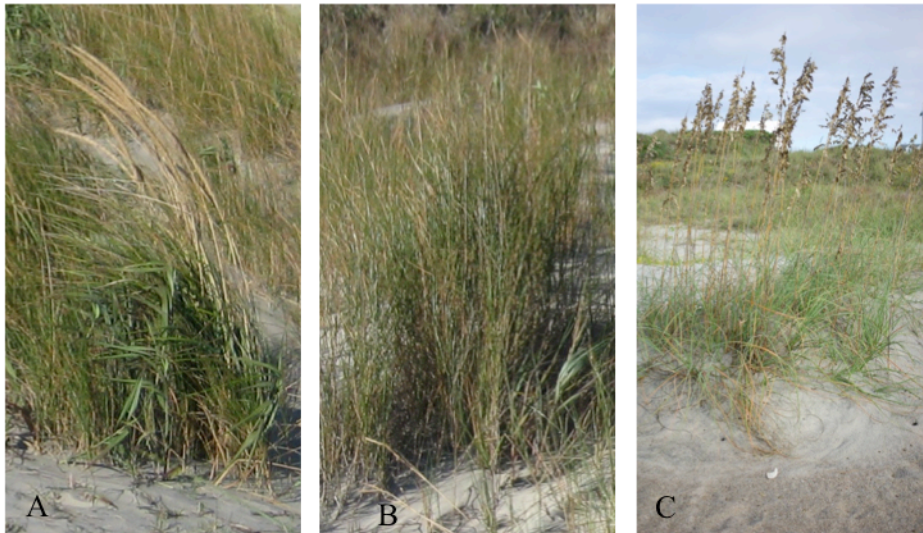
Figure 1. Species of interest in this experiment. *Ammophila breviligulata* (A), *Spartina patens* (B), and *Uniola paniculata* (C).
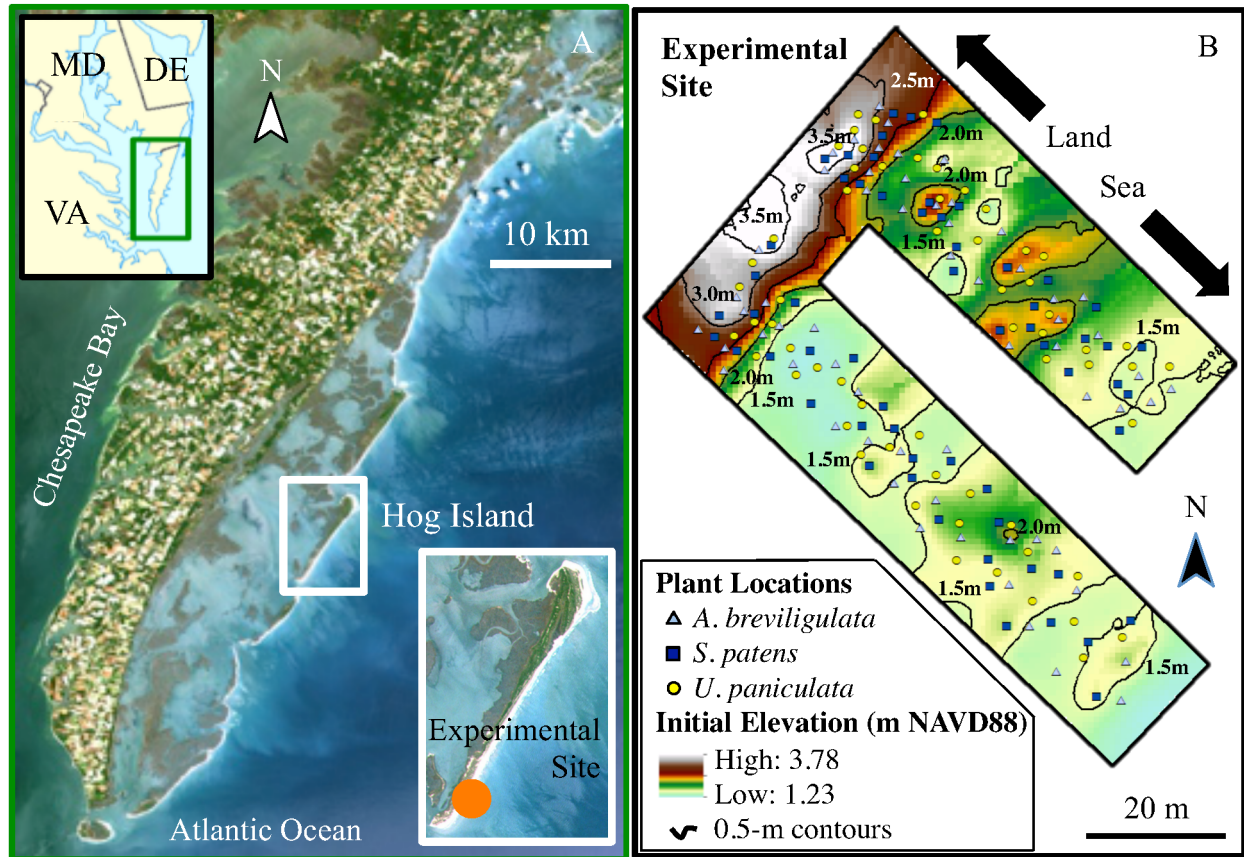
Figure 2. Experimental site maps. Location of experimental site on Hog Island in larger geographic area (A, NASA Thematic Mapper LANDSAT 7 Thematic Mapper Scene of Virginia Portion of the Delmarva Peninsula – 1999, data available at www.usgs.gov and vcrlter.virginia.edu) and locations and initial elevations (NAVD88) of individual plants within experimental site (B).
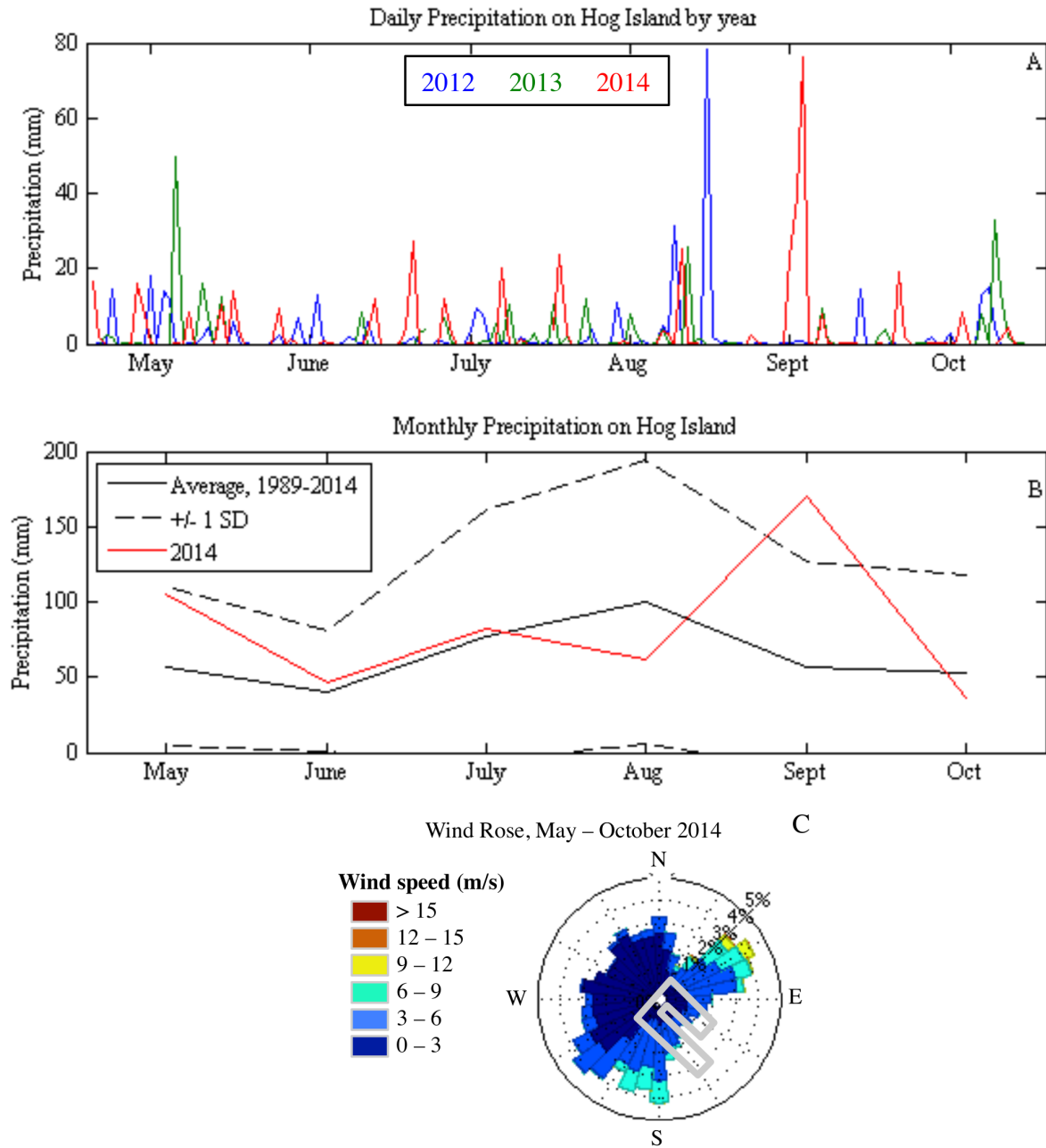
Figure 3. Hog Island 2014 weather. Daily (A) and monthly (B) precipitation, along with hour-averaged wind rose showing direction of wind origin (C) at Hog Island weather station (data from Porter et al. 2014a). Outline of experimental site overlays wind rose in gray. Time series start on May 21st (day of transplanting) and end on October 14th (last field observation). Plot in C generated using Matlab Central File Exchange file "WindRose" by Daniel Pereira (2015); file retrieved May 1, 2015.
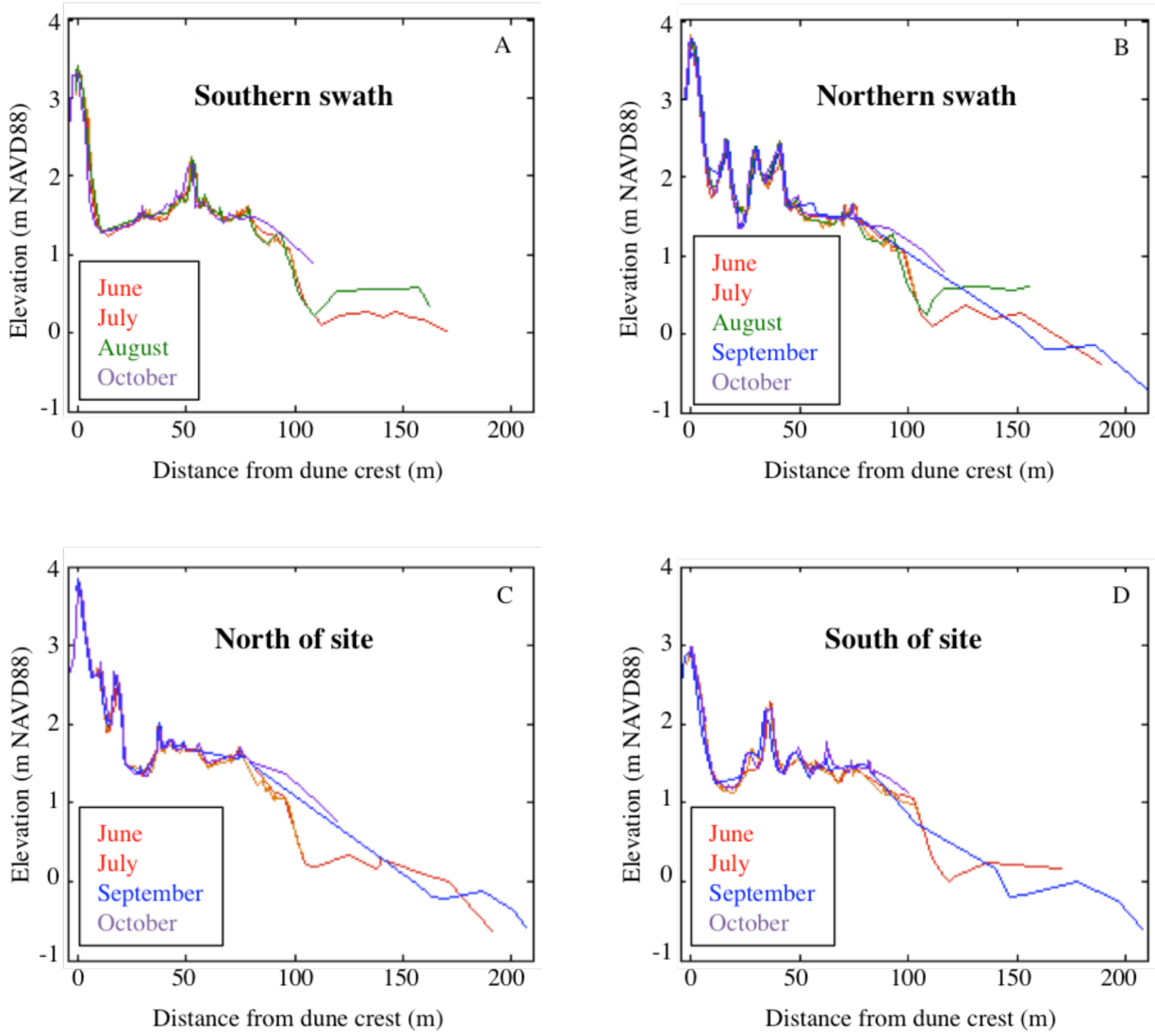
Figure 4. Monthly cross-shore beach profiles. Cross-shore beach profiles surveyed monthly along lines in southern transect (a), northern transect (b), south of experimental site (c), and north of experimental site (d). Locations on experimental site shown in Figure 5. Red tones represent early part of the record and blue tones represent the later part. Note areas of accretion likely due to subaqueous onshore sand transport after the September 10 HWE (x= ~100-120 m), changes in protodune elevation (x= ~10-75m), and channel cut in September (x= 24 m).
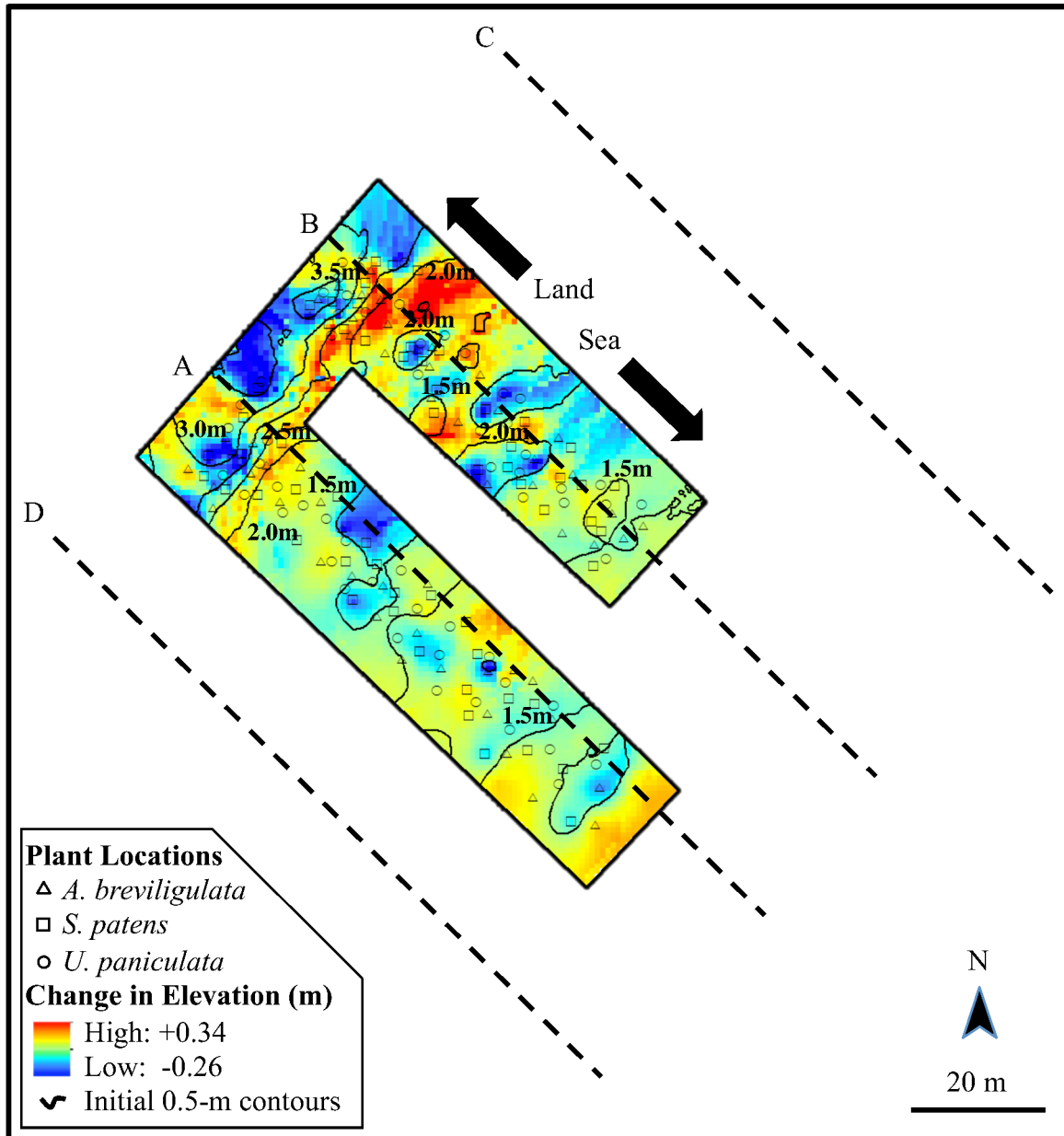
Figure 5. Topographic change within experimental site. Change in elevation in the experimental site from beginning to end of field season (June to October). Approximate locations of beach profiles shown in dashed lines.
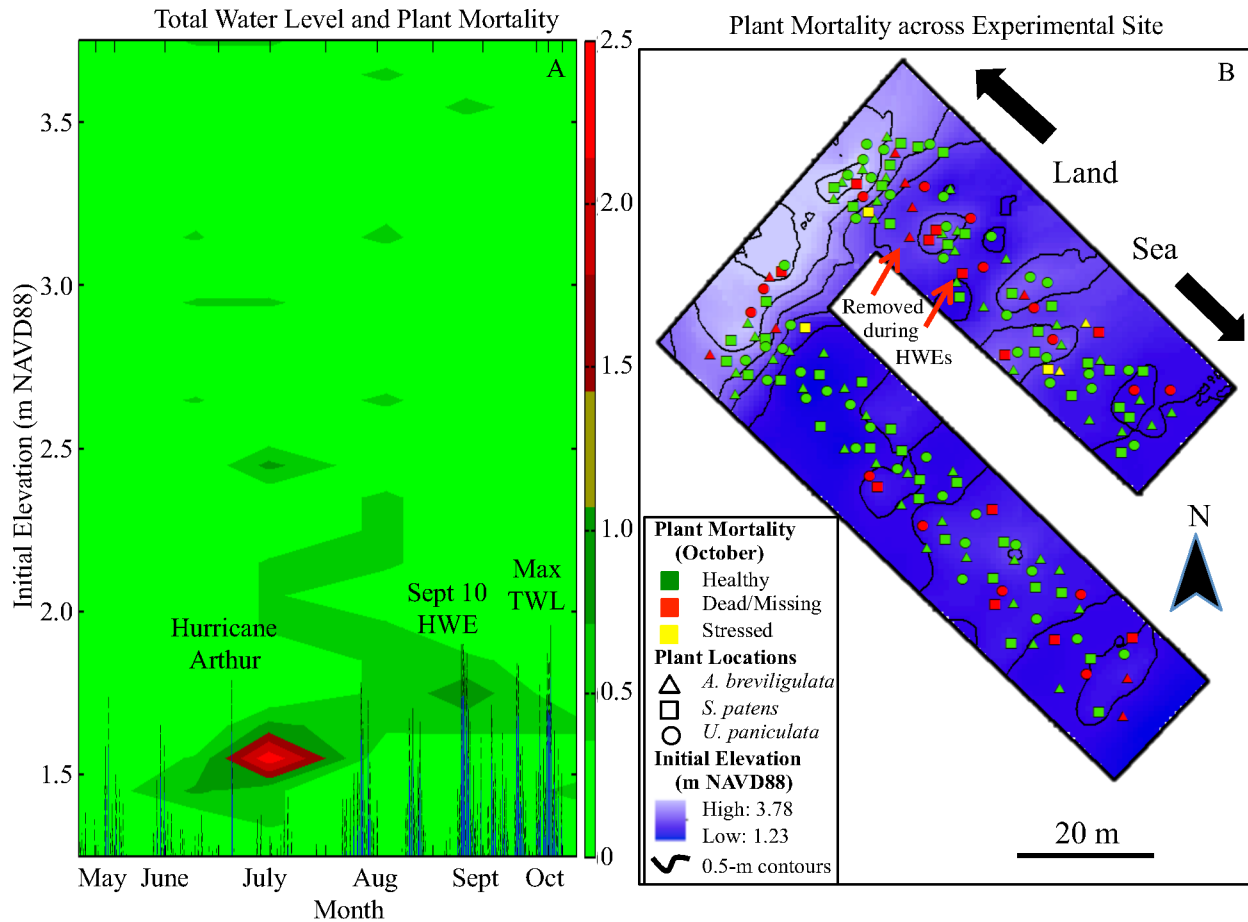
Figure 6. Plant mortality. A. Plant mortality vs. Total water level. Percentage of missing or dead plants compared to the total number of plants in previous month. Missing or dead plants are shown at the elevation and date on which they were first observed to be missing or dead, and then are removed from future calculations. Total Water Level (calculated as in Ruggiero et al. 2001) at Hog Island over 2014 experimental season calculated from tide gauge on Hog Island is overlain in blue, with tide gauge error in black dashes. B. Cumulative plant mortality across experimental site as of October 2014. Note high mortality along the edge of each swath and at the edge of protodunes, as well as locations of plants removed in HWEs (mentioned in Discussion).
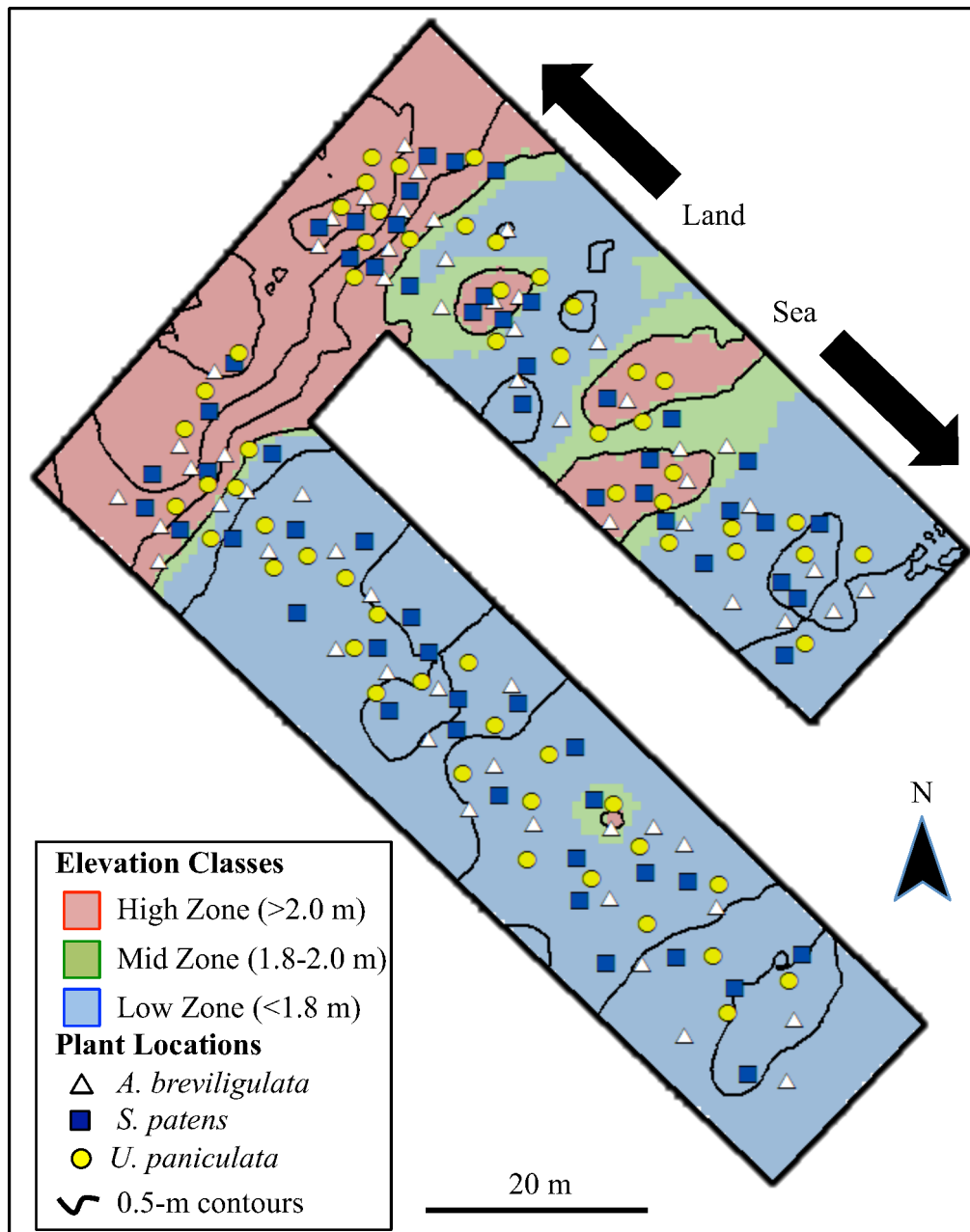
Figure 7. Elevation classification map. Plant locations in each elevation classification zone based on the maximum total water level in the growing season.
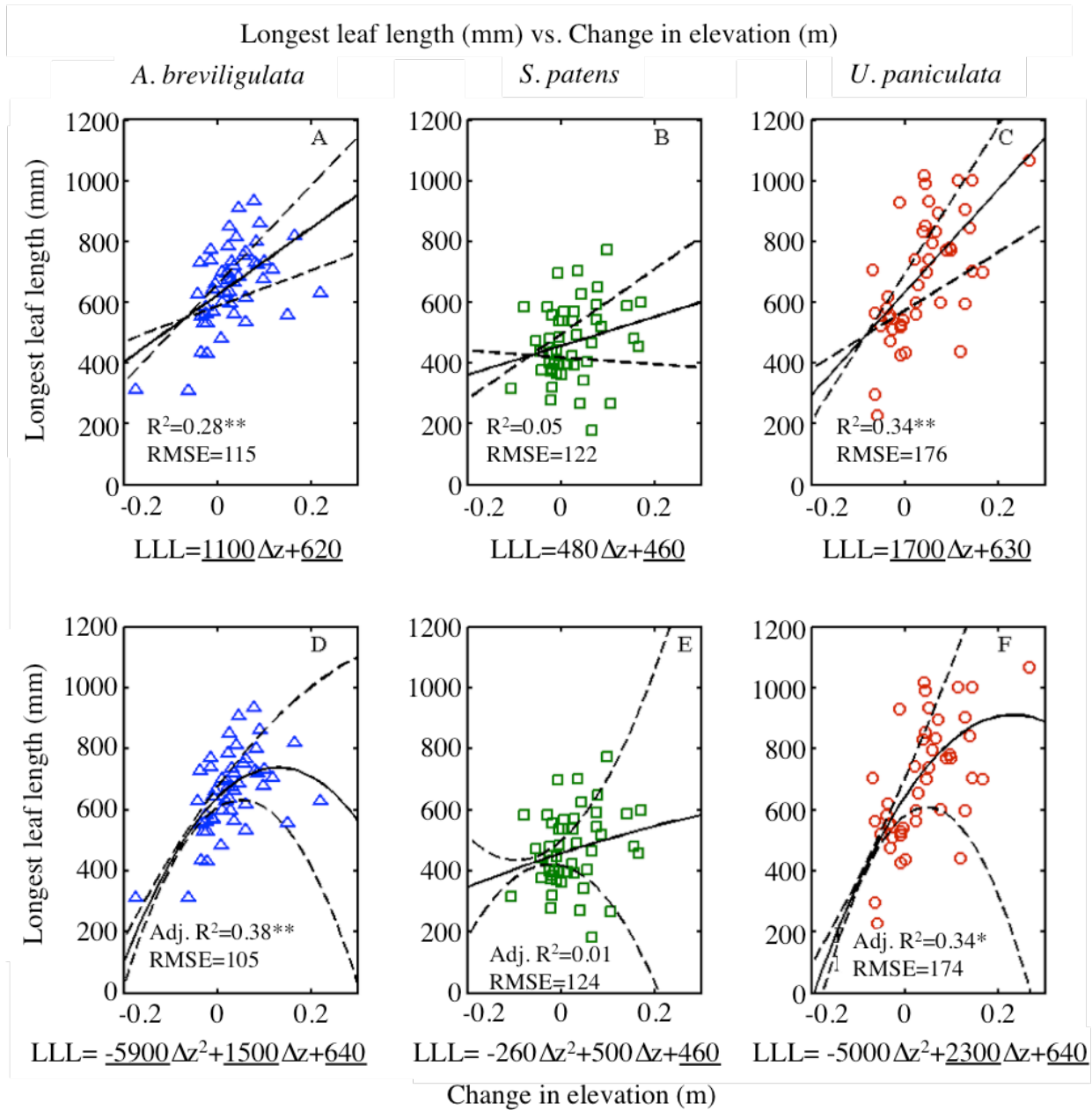
Figure 8. Longest leaf length vs. change in elevation. Transplant longest leaf length (mm) in *A. breviligulata* (A, D), *S. patens* (B, E), and *U. paniculata* (C, F) as a function of change in elevation (m). Linear regression (A-C), quadratic regression (D-F) equations underneath panels and represented by solid lines, with 95% confidence intervals in dashed lines. Relationships with all coefficients significant at the p<0.01 level marked with **; relationships with fewer than all coefficients significant at the p<0.05 level marked with *; significant coefficients underlined.
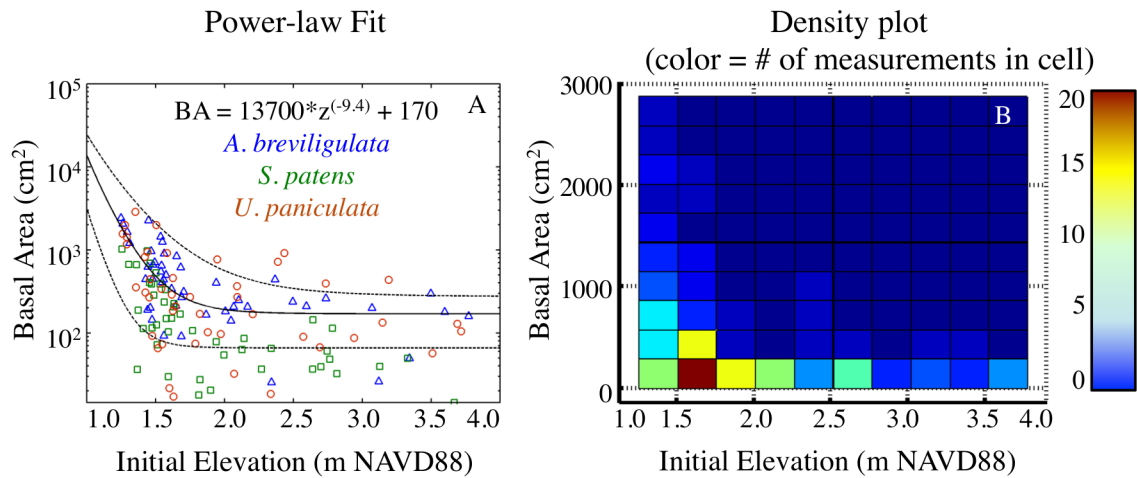
Figure 9. Basal area vs. Initial elevation. A. Nonlinear relationship between basal area and initial elevation. Regression line is solid, dashed lines are 95% confidence intervals. Adjusted R^2 = 0.47, RMSE=387. B. Density plot of basal area and initial elevation. Color scale represents number of plants within each grid cell.
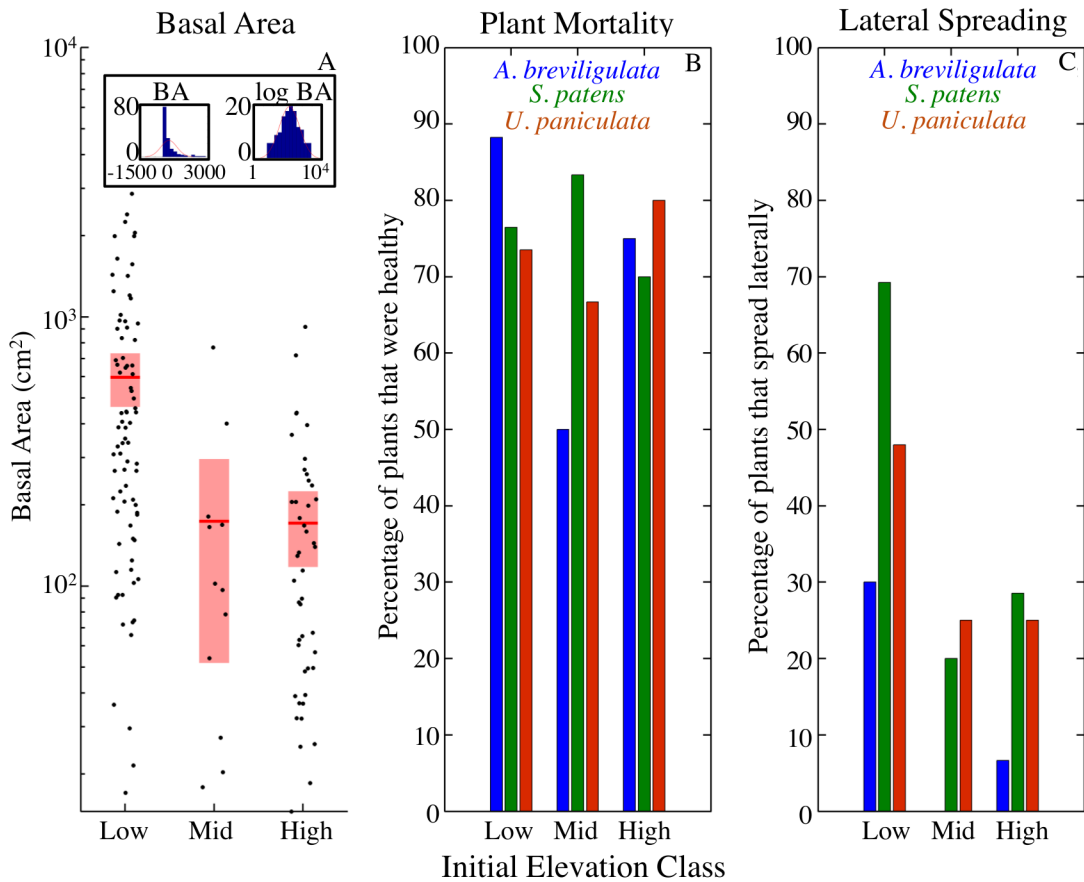
Figure 10. Categorical plant growth comparisons. Plant Log basal area (A, p<0.01), Health (B, p=0.47), and Spreading (C, p<0.01) across species in each elevation classification based on maximum total water level for growing season. Panel A: Red line= mean, red shade= 95% CI, black dots= data points. Histograms in panel A inset show untransformed basal area and log-transformed basal area. Plot in A generated using Matlab Central File Exchange file "notBoxPlot" by Rob Campbell (2010); file retrieved December 4, 2014.

Figure 11. Measurement and modeling of ratio of basal-to-frontal area. A. Ratio of basal-to-frontal area for each species by date compared to previous parameterization. Means for each group reported at top. B. Maximum dune height as a function of the ratio of basal-to-frontal area (BA/FA) ratio and *m* parameter. Note the nonlinear behavior at BA/FA= ~1 to 1.5 and that the BA/FA ratio resulting in maximum dune height is at BA/FA=0.8 when *m*= 0.16 and changes with parameter *m*. Plot in A generated using Matlab Central File Exchange file "notBoxPlot" by Rob Campbell (2010); file retrieved December 4, 2014.

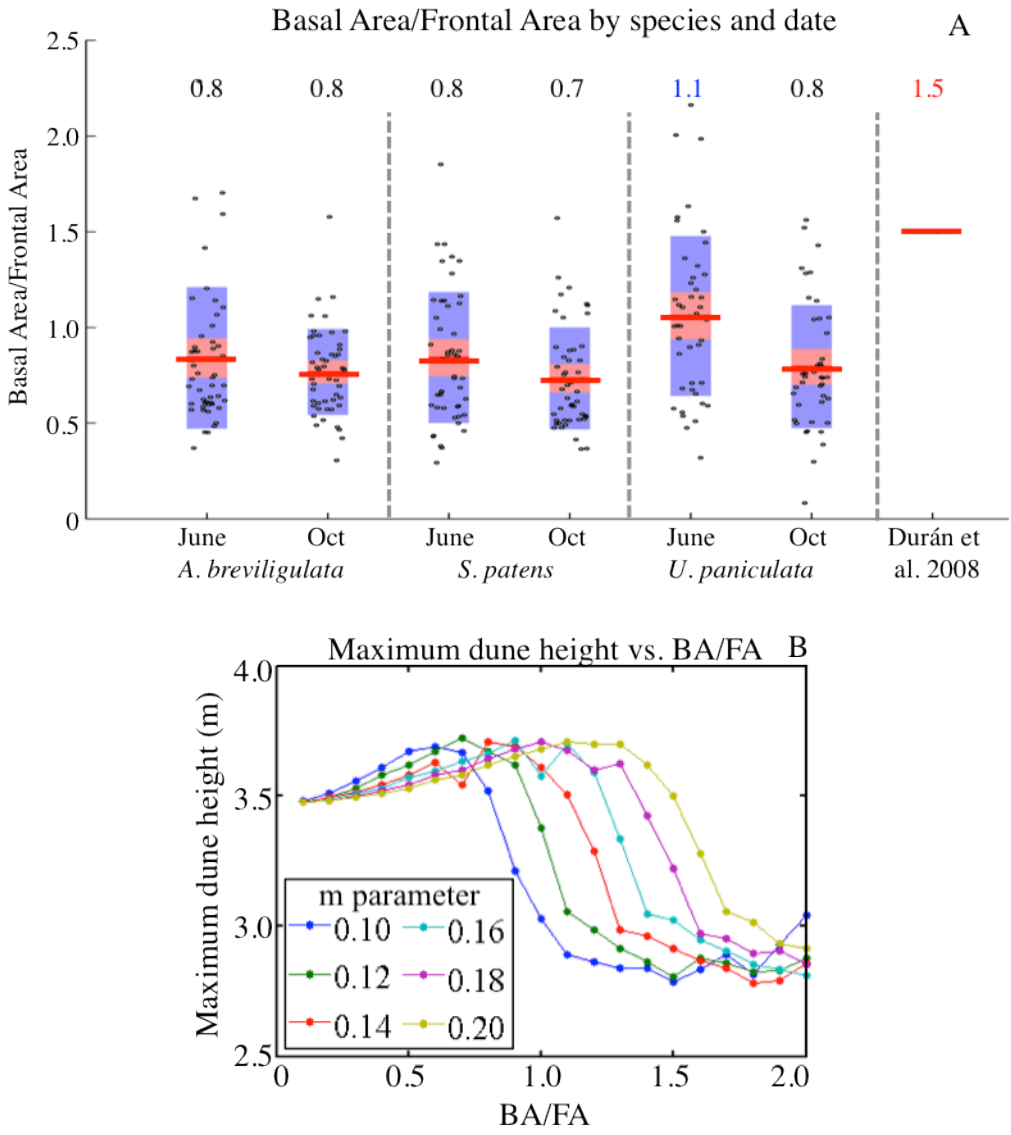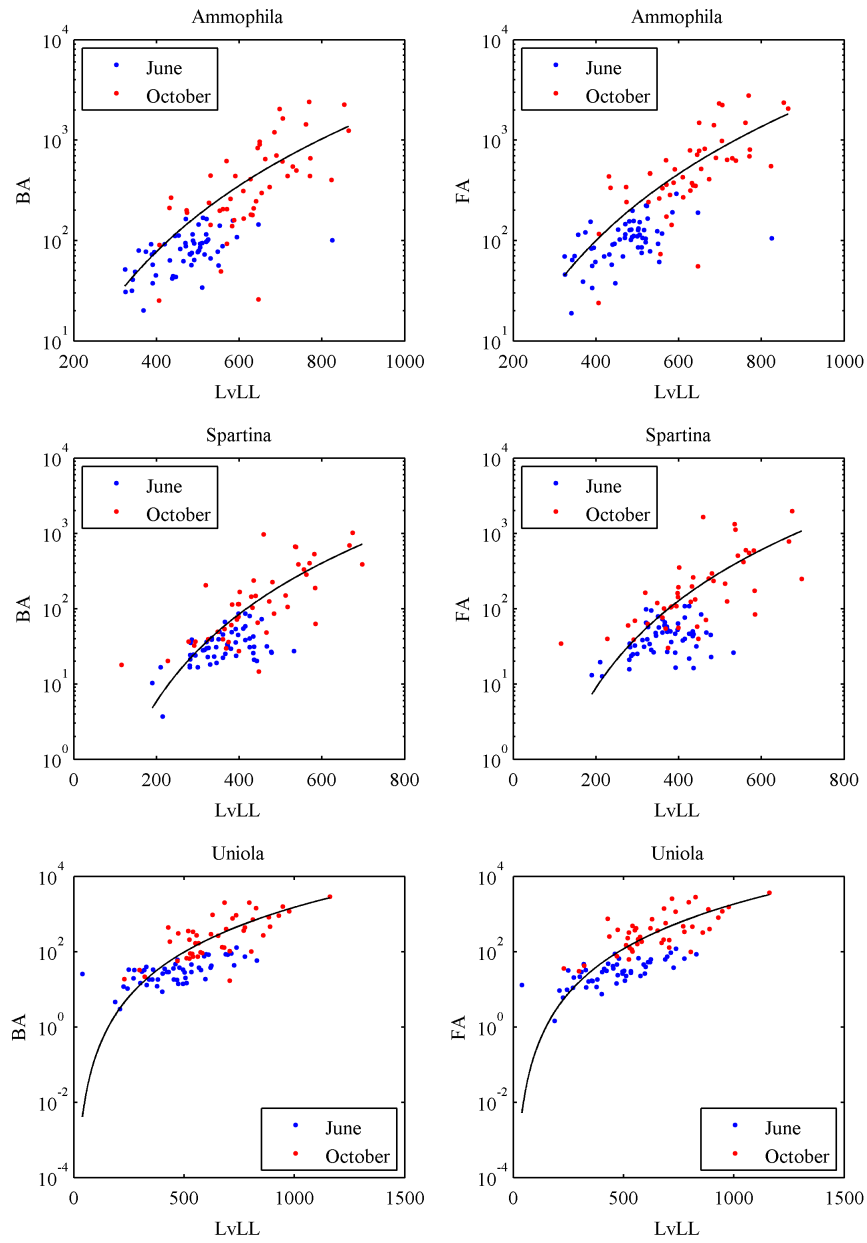**Figure 12. Allometric relationships between longest visible leaf length, basal area, and frontal area.** Allometric relationships between longest visible leaf length (LVLL, [mm]) and basal and frontal area (BA, FA [cm^2]) for each species.

APPENDIX 1: SUPPLEMENTARY METHODS

1.1 Experimental setup

I coded each plant according to its location. For example, the plant labeled "SB16L" is the leftward plant as one faces the dune (southernmost plant) at the 16th *S. patens* site from the shoreline on the northern swath, while the plant labeled "UA3R" is the rightward plant as one faces the dune (northernmost plant) at the 3rd *U. paniculata* site from the shoreline on the southern swath.

Two noteworthy meteorological events occurred at my experimental site during the 2014 growing season. First, the eye of Hurricane Arthur passed approximately 150 km to the south of my experimental site on July 4, 2014, bringing winds of 11.5 m/s to Hog Island (Porter et al. 2014a), 90 mph at the eye wall, and 45 mph at the NOAA Wallops Island Station, 65 km north of my experimental site. Second, an intense rainfall event over September 7-9 (138.38 mm of rain over the 3 days, Porter et al. 2014a) and an astronomical spring high tide combined to generate one of the highest high water events observed throughout the field season in my experimental site. Rainfall on September 9, 2014, at the NOAA meteorological station in nearby Norfolk, VA, recorded the highest 24-hour rainfall total on record (NOAA online data http://www.erh.noaa.gov/er/akq/climate/ORF_Climate_Records.pdf)

Initial topography within the experimental site ranged from 1.25 to 3.78 m. The highest elevations were on the foredune ridge, whereas the lowest were at the foredune toe and the seaward edge of transect A (the southernmost swath). The closest plant to the shoreline was plant AA1, at a distance of 21.3 m, while the furthest plant from the shoreline was AA29, at a distance of 103.5 m. There were two protodunes located on transect B (northern swath) at approximately 50 to 70 m and 80 to 85 m from the shoreline, having maximum elevations of 2.4 and 2.5 m,

respectively. Additionally, there was a single, smaller protodune on transect A (maximum elevation of 2.0 m) between 40 and 50 m from the shoreline (Figure 1B).

1.2 Measurements

I made a series of measurements and observations (longest leaf, plant state and elevation) monthly from June to October in 2014. To measure longest leaf length, I collected all the leaves of the plant, raised my hands to allow the shortest leaves to fall out, and then grasped the last leaf remaining. I placed a meter stick with an attached metal 90-degree joint on the sand surface and touching the base of the longest leaf, then recorded leaf length to the nearest millimeter. One lab member measured plants while another recorded the data. I measured plant mortality, or "plant state," by visually observing the color, uprightness, and number of each plant's leaves, as well as the presence or absence of each plant. Plants were then classified as "Healthy," "Stressed," "Dead," or "Missing," and I collected photographs of each plant for additional evidence of plant state (Figures S1-S3).

To measure elevation, I installed two GPS monuments landward of the experimental site, on the secondary dune ridge where sand conditions are less dynamic, and collected their UTM coordinates and NAVD88 elevations with a static survey. I then set a total station over one point, used the other as a backsight, and placed a prism set on a 2-meter pole with a wide-based topo shoe attached adjacent to the fiberglass stakes marking each plant to survey the elevation at each plant. I also collected four monthly cross-shore beach profiles along repeated transect lines by marking each profile's line with three fiberglass stakes, then laying a 100-meter measuring tape along the line delineated by the three stakes, then using the total station to collect a point at each change in slope (inflection point) along the profile. Profiles passed through the southern swath ("TA"), the northern swath ("TB"), north of the northern swath ("TN"), and south of the

southern swath ("TS") (Figure 5). Beach profiles started at the primary foredune crest and terminated at the water line; for this reason, each profile does not end at the same distance from the dune.

Salinity of the water sample was measured in the lab with a Hanna Instruments 98130 pH/conductivity/salinity/Total Dissolved Solids meter.

To measure the basal and frontal area of each plant, I photographed each plant in the plan (basal) and front (frontal) view in June and October. I set a black poster board behind the plant being measured to block background vegetation out of the photo and reduce wind around the plant, and set a clipboard in the photo including a pre-measured straight line for scale. Using the ImageJ software package, I measured the scale bar, removed as much background as possible, and then adjusted the color threshold using the HSV sliders and the Percentile method, until only the plant was highlighted. I then selected the highlighted area, and used the Measure tool in ImageJ to calculate the plant area in square centimeters (Figure S5).

S. patens

LLL = A + Bz + CΔz			
Coefficient	**Value**	**95% CI (+/-)**	**t-statistic**
A**	600	120	9.9
B*	-80	65	-2.5
C*	830	630	2.7
N= 48, DOF= 45, RMSE= 116, R^2= 0.17, Adj. R^2= 0.13			
F-statistic vs. constant model: 4.6, p = 0.01			

LLL = A + Bx + CΔz			
Coefficient	**Value**	**95% CI (+/-)**	**t-statistic**
A**	620	120	11
B**	-2.4	1.6	-3.0
C*	800	580.0	2.7
N= 48, DOF= 45, RMSE= 113, R^2= 0.21, Adj. R^2= 0.18			
F-statistic vs. constant model: 6.0, p < 0.01			

LLL = A + Bz + Cx + DΔz			
Coefficient	**Value**	**95% CI (+/-)**	**t-statistic**
A**	660	130	9.9
B	-41	76	-1.1
C	-1.8	2.0	-1.9
D**	900	620	2.9
N= 48, DOF= 44, RMSE= 113, R^2= 0.23, Adj. R^2= 0.18			
F-statistic vs. constant model: 4.4, p = 0.01			

Table S1. Multiple linear regression with *S. patens*. Comparison among three possible fit equations relating longest leaf length (mm) to environmental parameters (m) in *S. patens*. Coefficients, 95% confidence intervals, and the t-statistic for each variable are shown, with p values <0.05 marked with * and p values <0.01 marked with **. Goodness-of-fit statistics (Number of replicates (N), Degrees of freedom (DOF), Root mean square error (RMSE), R^2, Adjusted R^2) and the F-statistic and p-value for the overall fit equation at bottom.

$$\textbf{LLL = A + Bz + Cx}$$

A. breviligulata			
Coefficient	**Value**	**95% CI (+/-)**	**t-statistic**
A**	670	140	9.4
B	12	74	0.3
C	-0.6	2.3	-0.5
N= 50, DOF= 47, RMSE= 136, R^2= 0.01, Adj. R^2<0.01			
F-statistic vs. constant model: 0.1, p = 0.88			

S. patens			
Coefficient	**Value**	**95% CI (+/-)**	**t-statistic**
A**	590	130	8.8
B	-7.8	8.8	-0.2
C	-1.4	2.1	-1.4
N= 48, DOF= 45, RMSE= 122, R^2= 0.08, Adj. R^2= 0.04			
F-statistic vs. constant model: 1.9, p = 0.16			

U. paniculata			
Coefficient	**Value**	**95% CI (+/-)**	**t-statistic**
A**	590	240	4.9
B	-70	120	-1.2
C	3.3	3.7	1.8
N= 45, DOF= 42, RMSE= 211, R2= 0.07, Adj. R^2= 0.03			
F-statistic vs. constant model: 1.7, p = 0.20			

Table S2. Multiple linear regression with distance to shoreline and initial elevation only.

Possible fit equations relating longest leaf length (mm) to distance to shoreline and initial

elevation (m) in each species. Coefficients, 95% confidence intervals, and the t-statistic for each

variable are shown, with p values <0.05 marked with * and p values <0.01 marked with **.

Goodness-of-fit statistics (Number of replicates (N), Degrees of freedom (DOF), Root mean

square error (RMSE), R^2, Adjusted R^2) and the F-statistic and p-value for the overall fit equation

at bottom.

LLL = A + Bz + Cx + DΔz

A. breviligulata			
Coefficient	**Value**	**95% CI (+/-)**	**t-statistic**
A**	720	120	12
B	-23	64	-0.7
C	-0.8	1.9	-0.9
D**	1200	540	4.6
N= 50, DOF= 46, RMSE= 114, R^2= 0.32, Adj. R^2= 0.27			
F-statistic vs. constant model: 7.2, $p < 0.01$			

S. patens			
Coefficient	**Value**	**95% CI (+/-)**	**t-statistic**
A**	660	130	9.9
B	-41	76	-1.1
C	-1.8	2.0	-1.9
D**	900	620	2.9
N= 48, DOF= 44, RMSE= 113, R^2= 0.23, Adj. R^2= 0.18			
F-statistic vs. constant model: 4.4, $p = 0.01$			

U. paniculata			
Coefficient	**Value**	**95% CI (+/-)**	**t-statistic**
A**	640	190	6.8
B**	-138	93	-3.0
C*	3.4	2.8	2.4
D**	1900	710	5.5
N= 45, DOF= 41, RMSE= 162, R2= 0.47, Adj. R^2= 0.43			
F-statistic vs. constant model: 12, $p < 0.01$			

Table S3. Multiple linear regression with all environmental parameters. Possible fit equations relating longest leaf length (mm) to environmental parameters (m) in each species. Coefficients, 95% confidence intervals, and the t-statistic for each variable are shown, with p values <0.05 marked with * and p values <0.01 marked with **. Goodness-of-fit statistics (Number of replicates (N), Degrees of freedom (DOF), Root mean square error (RMSE), R^2, Adjusted R^2) and the F-statistic and p-value for the overall fit equation at bottom.

$$\text{LLL} = A + Bz + Cx + D\Delta z + E\Delta z^2$$

A. breviligulata			
Coefficient	**Value**	**95% CI (+/-)**	**t-statistic**
A**	720	110	13
B	-4.6	60	-0.2
C	-1.1	1.7	-1.2
D**	1600	560	5.8
E**	-5800	3800	-3.1
N= 50, DOF= 45, RMSE= 105, R^2= 0.44, Adj. R^2= 0.39			
F-statistic vs. constant model: 8.7, $p < 0.01$			
S. patens			
Coefficient	**Value**	**95% CI (+/-)**	**t-statistic**
A**	660	140	9.9
B	-49	79	-1.2
C	-1.8	2.0	-1.8
D	720	800	1.8
E	2600	7200	0.7
N= 48, DOF= 43, RMSE= 114, R^2= 0.24, Adj. R^2= 0.17			
F-statistic vs. constant model: 3.4, $p = 0.02$			
U. paniculata			
Coefficient	**Value**	**95% CI (+/-)**	**t-statistic**
A**	660	190	6.8
B*	-130	94	-2.8
C*	3.1	3.0	2.1
D**	2300	1100	4.1
E	-3000	7000	-0.9
N= 45, DOF= 40, RMSE= 162, R2= 0.48, Adj. R^2= 0.42			
F-statistic vs. constant model: 9.0, $p < 0.01$			

Table S4. Multiple linear regression with all environmental parameters and quadratic change in elevation. Possible fit equations relating longest leaf length (mm) to environmental parameters (m) in each species. Coefficients, 95% confidence intervals, and the t-statistic for each variable are shown, with p values <0.05 marked with * and p values <0.01 marked with **. Goodness-of-fit statistics (Number of replicates (N), Degrees of freedom (DOF), Root mean square error (RMSE), R^2, Adjusted R^2) and the F-statistic and p-value for the overall fit equation at bottom.

A. breviligulata

$LLL = A + Bz + Cx + D\Delta z + E\Delta z^2$			
Coefficient	**Value**	**95% CI (+/-)**	**t-statistic**
A**	750	110	14
B	-18	63	-0.6
C	-1.3	1.6	-1.6
D**	2500	1000	4.8
E	-9600	15000	-1.2
N= 46, DOF= 41, RMSE= 96, R^2= 0.47, Adj. R^2= 0.42			
F-statistic vs. constant model: 9.1, $p < 0.01$			
$LLL = A + B\Delta z$			
Coefficient	**Value**	**95% CI (+/-)**	**t-statistic**
A**	620	33	36
B	1700	690	4.8
N= 48, DOF= 43, RMSE= 114, R^2= 0.24, Adj. R^2= 0.17			
F-statistic vs. constant model: 3.4, $p = 0.02$			

Table S5. Multiple linear regression with *A. breviligulata* and large Δz values removed.

Possible fit equations relating longest leaf length (mm) to environmental parameters (m) in *A. breviligulata* when data points with four most extreme Δz values are removed. Coefficients, 95% confidence intervals, and the t-statistic for each variable are shown, with p values <0.05 marked with * and p values <0.01 marked with **. Goodness-of-fit statistics (Number of replicates (N), Degrees of freedom (DOF), Root mean square error (RMSE), R^2, Adjusted R^2) and the F-statistic and p-value for the overall fit equation at bottom.

Figure S1. Plant mortality in *A. breviligulata*. *A. breviligulata* transplants classified as Healthy (A, plant AA3), Stressed (B, plant AB7), Dead (C, plant AB12), and Missing (D, plant AA29) in October.

Figure S2. Plant mortality in *S. patens*. *S. patens* transplants classified as Healthy (A, plant SA3), Stressed (B, plant SB8), Dead (C, plant SA4), and Missing (D, plant SA2) in October.

Figure S3. Plant mortality in *U. paniculata*. *U. paniculata* transplants classified as Healthy (A, plant UA11, October), Stressed (B, plant UB14, August), Dead (C, plant UA4, August), and Missing (D, plant UA12, October).
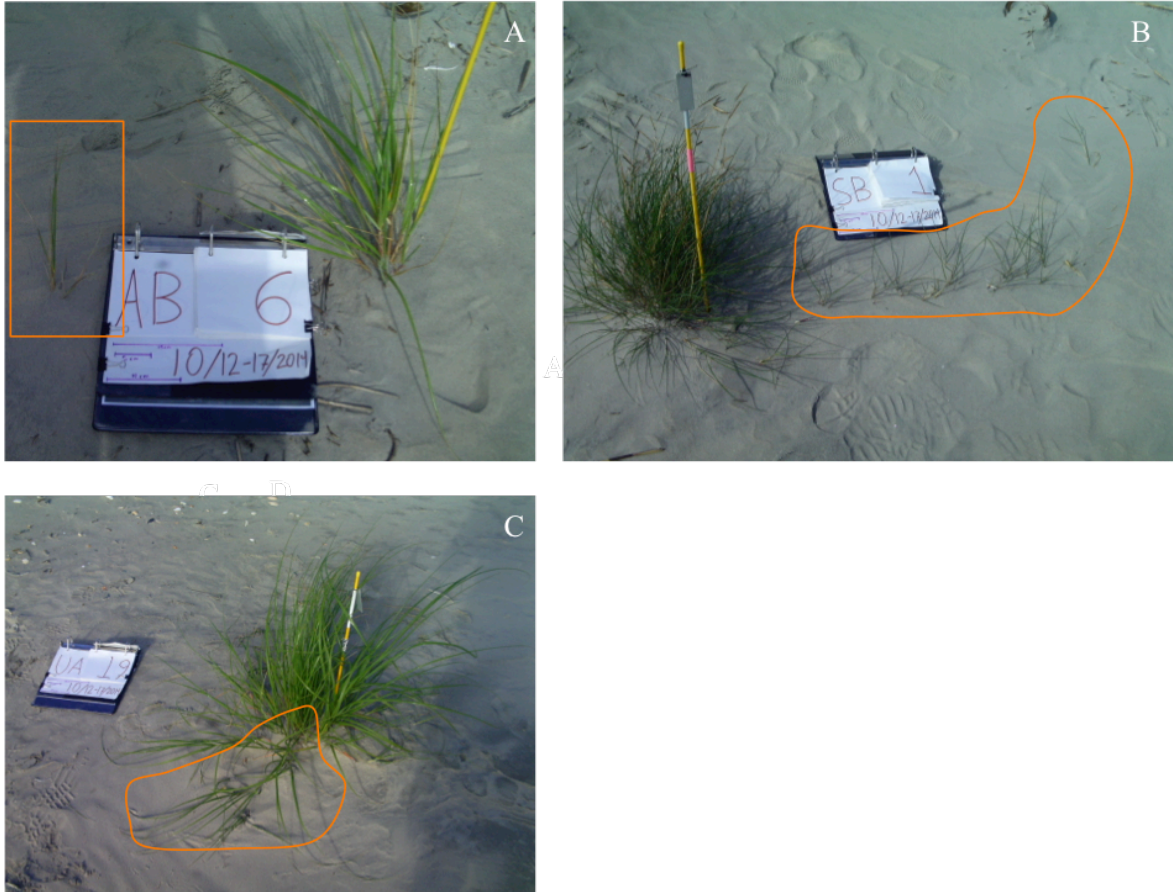
Figure S4. Lateral spreading in each species. Lateral spreading in *A. breviligulata* (A, plant

AB6) *S. patens* (B, plant SB1), and *U. paniculata* (C, plant UA19) in October. New shoots and

spreading centers are highlighted in orange.
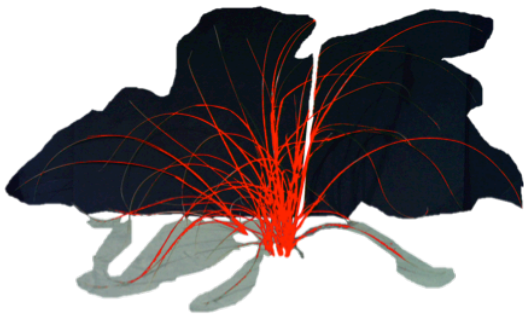
Figure S5. Basal and frontal area measurements. Steps in frontal area measurement of plant UB5: photography (A), cropping (B), thresholding (C), and measurement (D). Basal area measurements are equivalent, but with plan-view photography.

Figure S6. Longest leaf length vs. initial elevation and distance to shoreline. Transplant growth, measured by longest leaf length, in *A. breviligulata* (blue; A, D), *S. patens* (green; B, E), and *U. paniculata* (red; C, F) as a function of initial elevation (m NAVD88; A-C) and distance to shoreline (m from MHW; D-F). Regression equations are underneath each panel and represented by solid lines, with 95% confidence intervals in dashed lines. None of these relationships were significant at the p=0.05 confidence level.
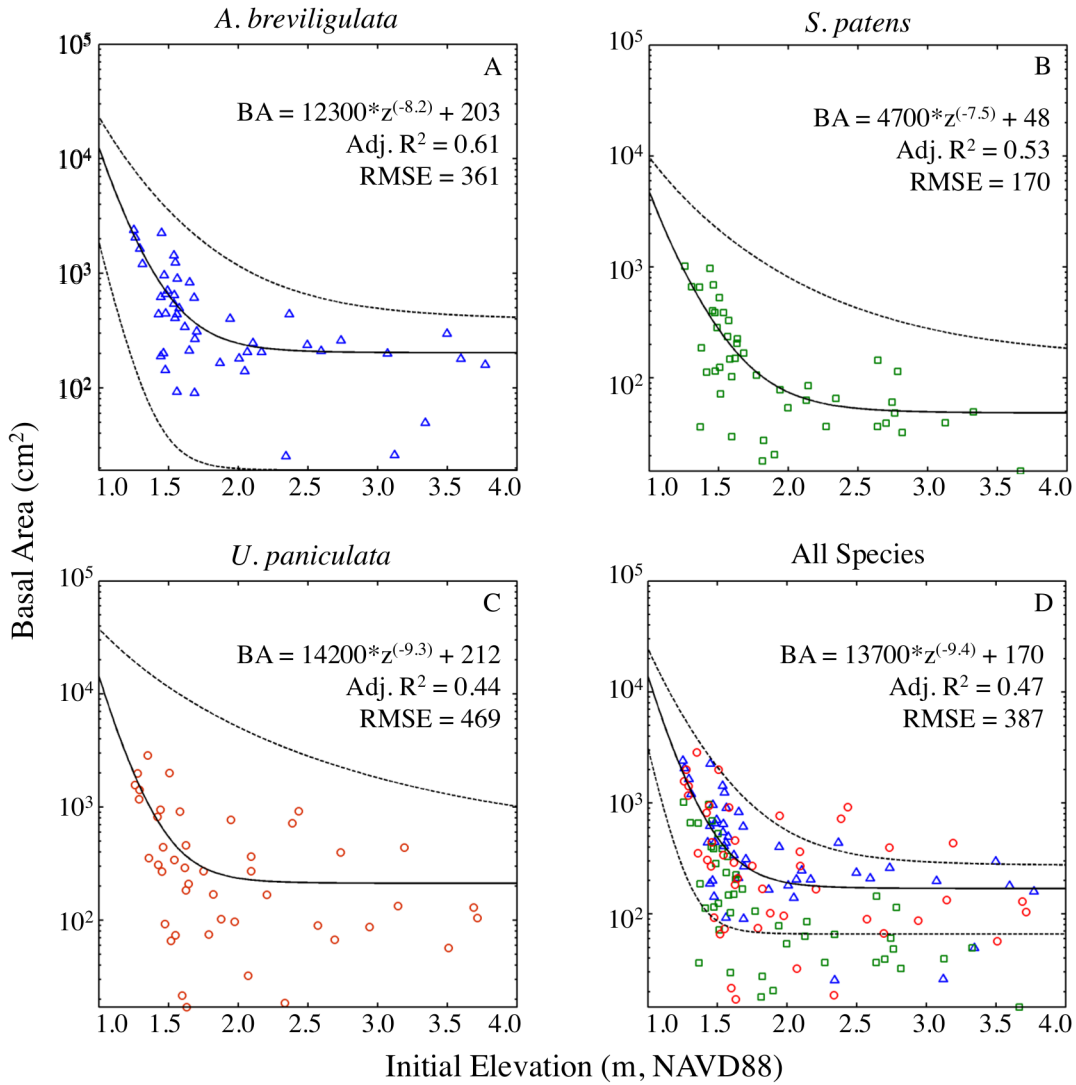
Figure S7. Basal area vs. initial elevation with power-law equations. Basal area vs. initial elevation with power-law ($y = A*x^b + c$) fit equations for each species, and for all species together.
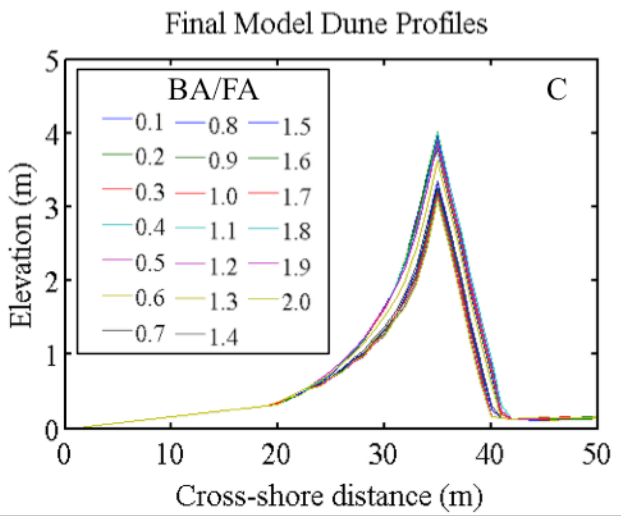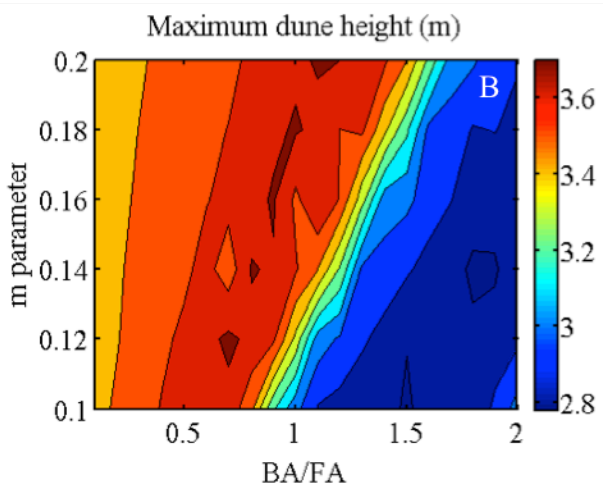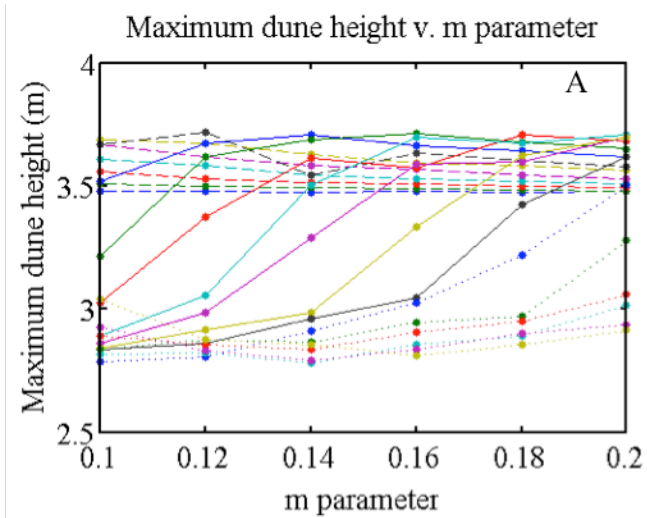
Figure S8. Maximum dune height as function of basal-to-frontal area and m parameter.

Maximum modeled dune height as function of m parameter and basal-to-frontal area ratio (A, B),

and final modeled dune profiles as a function of basal-to-frontal area ratio.

REFERENCES

Anderson, L.C. and Alexander, L.L. 1985. The vegetation of Dog Island Florida. Florida Scientist 48 (4): 232-251.

Arens, S.M., Baas, A.C.W., van Boxel, J.H., and Kalkman, C. 2001. Influence of reed stem density on foredune development. Earth Surface Processes and Landforms 26: 1161-1176.

Barbier, E.B. et al. 2011. The value of estuarine and coastal ecosystems. Ecological Monographs 81: 169-193.

Barbour, M.G. and De Jong, T.M. 1977. Response of west coast beach taxa to salt spray, seawater inundation, and soil salinity. Bulletin of the Torrey Botanical Club 104: 29-34.

Bertness, M.D. and Callaway, R. 1994. Positive interactions in communities. Trends in Ecology and Evolution 9: 191-193.

Bindoff, N.L., Willebrand, J., Artale, V., Cazenave, A., Gregory, J., Gulev, S. et al. 2007. Observations: Oceanic Climate Change and Sea Level. In Solomon, S., Qin, D., Manning, M., Chen, Z., Marquis, M., Averyt, K.B. et al. (eds.): Climate Change 2007: The Physical Science Basis. Contribution of Working Group I to the Fourth Assessment Report of the Intergovernmental Panel on Climate Change. Cambridge University Press, Cambridge, United Kingdom and New York, NY, USA.

Brantley, S.T., Bissett, S.N., Young, D.R., Wolner, C.W.V., and Moore, L.J. 2014. Barrier island morphology and sediment characteristics affect the recovery of dune building grasses following storm-induced overwash. PLOS ONE. doi: 10.1371/journal.pone.0104747.

Borsje, B.W., van Wesenbeck, B.K., Dekker, F., Paalvast, P., Bouma, T.J., van Katwijk, M.M. et al. 2011. How ecological engineering can serve in coastal protection. Ecological Engineering 37 (2): 113-122.

Burdick, D.M. 1989. Root aerenchyma development in *Spartina patens* in response to flooding. American Journal of Botany 75 (5): 777-780.

Burdick, D.M. and Mendelssohn, I.A. 1987. Waterlogging responses in dune, swale and marsh populations of *Spartina patens* under field conditions. Oecologia 75 (3): 321-329.

Castanho, C.d.T., Lortie, C.J., Zaitchik, B., and Prado, P.I. 2015. A meta-analysis of plant facilitation in coastal dune systems: responses, regions, and research gaps. PeerJ 3:e768. doi: 10.7717/peerj.768.

Church, J.A. and White, N.J. 2006. A 20th century acceleration in global sea-level rise. Geophysical Research Letters 33: 94-97.

Craig, R.M. 1975. Natural vegetation of Florida's coastal dunes. Proceedings of the Soil and Crop Society of Florida 34: 169-171.

Crossett, K., Culliton, T.J., Wiley, P., and Goodspeed, T.R. 2004. Population trends along the coastal United States, 1980-2008. Silver Spring, MD: National Oceanic and Atmospheric Administration.

Crowell, M., Edelman, S., Coulton, K., and McAfee, S. 2007. How many people live in coastal areas? Journal of Coastal Research 23 (5): iii-vi.

de Winter, R.C., Gongriep, F., and Ruessink, B.G.. 2015. Observations and modeling of alongshore variability in dune erosion at Egmond aan Zee, the Netherlands. Coastal Engineering. ISSN 0378-3839, http://dx.doi.org/10.1016/j.coastaleng.2015.02.005.

Dilustro, J.J. and Day, F.P. 1997. Aboveground biomass and net primary production along a Virginia barrier island dune chronosequence. American Midland Naturalist 137 (1): 27-38.

Durán, O. and Moore, L.J. 2013. Vegetation controls on the maximum size of coastal dunes. Proceedings of the National Academy of Sciences of the United States of America 110 (43): 17212-17222. doi: 10.1073/pnas.1307580110.

Durán, O. and Moore, L.J. 2015. Barrier island bistability induced by biophysical interactions. Nature Climate Change 5: 158-162. doi: 10.1038/nclimate2474.

Durán, O., Silva, M.V.N., Bezerra, L.J.C., Herrmann, H.J., and Maia, L.P. 2008. Measurements and numerical simulations of the degree of activity and vegetation cover on parabolic dunes in north-eastern Brazil. Geomorphology 102: 460-471.

Durán, O. and Herrmann, H.J. 2006. Vegetation against dune mobility. Physical Review Letters 97: 188001.

Ehrenfeld, J.G. 1990. Dynamics and processes of barrier island vegetation. Reviews in Aquatic Sciences 2: 437-480.

Everard, M., Jones, L., and Watts, B. 2010. Have we neglected the societal importance of sand dunes? An ecosystem services perspective. Aquatic Conservation: Marine and Freshwater Ecosystems 20: 476-487.

Fenster, M., and Dolan, R. 1994. Large-scale reversals in shoreline trends along the U.S. mid-Atlantic Coast. Geology 22: 543-546.

Forey, E., Chapelet, B., Vitasse, Y. Tilquin, M., Touzard, B., and Michalet, R. 2008. The relative importance of disturbance and environmental stress at local and regional scales in French coastal sand dunes. Journal of Vegetation Science 19 (4): 493-502.

Franks, S.J. 2003. Competitive and facilitative interactions within and between two species of coastal dune perennials. Canadian Journal of Botany 81 (4): 330-337.

Gilbert, M.E. and Ripley, B.S. 2010. Resolving the differences in plant burial responses. Austral Ecology 35: 53-59.

Godfrey, P.J. 1977. Climate, plant response and development of dunes on barrier beaches along United States east coast. International Journal of Biometeorology 21: 203–215.

Gurnell, A.M. et al. 2001. Riparian vegetation and island formation along the gravel-bed Fiume Tagliamento, Italy. Earth Surface Processes and Landforms 26: 31-62.

Hacker et al. 2011. Subtle differences in two non-native congeneric beach grasses significantly affect their colonization, spread, and impact. Oikos 121 (1): 138-148.

Harvill, A.M., Stevens, C.E. and Ware, D.M.E. 1977. Atlas of the Virginia flora, Part I. Pteridophytes through monocotyledons. Virginia Botanical Associates: Farmville, VA.

Hayden, B.P., Santos, M.C.F.V., Shao, G., and Kochel, R.C. 1995. Geomorphological controls on coastal vegetation at the Virginia Coast Reserve. Geomorphology 13: 283-300.

Hayes, M.O. 1979. Barrier island morphology as a function of tidal and wave regime. In Leatherman, S.P. (ed.). Barrier Islands. Academic Press: New York, 1-28.

He, Q., Bertness, M.D., and Altieri, A.H. 2013. Global shifts towards positive species interactions with increasing environmental stress. Ecology Letters 16: 695-706. doi: 10.111/ele.12080.

Hesp, P.A. 1989. A review of biological and geomorphological processes involved in the initiation and development of incipient foredunes. Proceedings of the Royal Society of Edinburgh 96B: 181-201.

Hesp, P.A. 1991. Ecological processes and plant adaptations on coastal dunes. Journal of Arid Environments 21: 165-191.

Hesp, P.A. 2002. Foredunes and blowouts: Initiation, geomorphology and dynamics. Geomorphology 48: 245–268.

Hesp, P.A. 2004. Coastal Dunes in the tropics and temperate regions: location, formation, morphology and vegetation processes. Ecological Studies 171: 29-49.

Hesp, P.A. 2013. A 34 year record of foredune morphodynamics, Dark Point, NSW, Australia. Journal of Coastal Research Special Issue 65: 1295-1300. doi: 10.2112/SI65-219.1.

Hester, M.W. and Mendelssohn, I.A. 1989. Water relations and growth responses of *Uniola paniculata* (sea oats) to soil moisture and water-table depth. Oecologia 78: 289-296.

Houston, J.R. 2008. The economic value of beaches: a 2008 update. Shore and Beach 76:22–26.

Keijsers, J.G.S., De Groot, A.V., and Riksen, M.J.P.M. 2015. Vegetation and sedimentation on coastal foredunes. Geomorphology 228: 723-734.

Knutson, T.R., Sirutis, J.J., Vecchi, G.A., Garner, S., Zhao, M., Kim, H.S., et al. 2013. Dynamical downscaling projections of Twenty-first-Century Atlantic hurricane activity: CMIP3 and CMIP5 model-based scenarios. Journal of Climate 26: 6591–6617. doi: http://dx.doi.org/10.1175/JCLI-D-12-00539.1.

Kobayashi, N., Raichle, A., and Asano, T. 1993. Wave attenuation by vegetation. Journal of Waterway, Port, Coastal, and Ocean Engineering 199 (1): 30-48.

Kuriyama, Y., Mochizuki, N., and Tsuyoshi, N. 2005. Influence of vegetation on aeolian sand transport rate from a backshore to a foredune at Hasaki, Japan. Sedimentology 52 (5): 1123-1132. doi: 10.111/j.1365-3091.2005.00734.x

Lane, C., Wright, S.J., Roncal, J, and Maschinski, J. 2008. Characterizing environmental gradients and their influence on vegetation zonation in a subtropical coastal sand dune system. Journal of Coastal Research 24 (4C): 213-224.

Martin, W.E. 1959. The vegetation of Island Beach State Park, New Jersey. Ecological Monographs 29 (1): 1-46.

Maun, M.A. and Perumal, J. 1999. Zonation of vegetation on lacustrine coastal dunes: effects of burial by sand. Ecology Letters 2: 14-18.

Maun, M.A. 2009. Biology of Coastal Sand Dunes. Oxford University Press: New York.

Miot da Silva, G., Hesp, P.A., Peixoto, J., Dillenburg, S.R. 2008. Foredune vegetation patterns and alongshore environmental gradients: Moçambique Beach, Santa Catarina Island, Brazil. Earth Surface Processes and Landforms 33: 1557-1573.

Möller, I. et al. 2014. Wave attenuation over coastal salt marshes under storm surges conditions. Nature Geoscience 7: 727-731. doi: 10.1038.ngeo2251.

Naidoo, G., McKee, K.L., and Mendelssohn, I.A. 1992. Anatomical and metabolic responses to waterlogging and salinity in *Spartina alterniflora* and *S. patens* (Poaceae). American Journal of Botany 79(7): 765-770.

Nordstrom, K.F., Lampe, R., Vandemark, L.M. 2000. Reestablishing naturally functioning dunes on developed coasts. Environmental Management 25 (1): 37-51.

Nordstrom, K.F. 2008. Beach and dune restoration. Cambridge University Press: New York.

Oosting, H.J., and Billings, W.D. 1942. Factors effecting vegetational zonation on coastal dunes. Ecology 23 (2): 131-142.

Pfeffer, W.T., Harper, J.T., and O'Neel, S. 2008. Kinematic constraints on glacier contributions to 21st-Century sea level rise. Science 321: 1340-1343.

Philip, J.R. 1973. Periodic nonlinear diffusion: An integral relation and its physical consequences. Australian Journal of Physics 26 (4): 513 – 520.

Porter, J., D. Krovetz, W. Nuttle, and J. Spitler. 2014. Hourly meteorological data for the Virginia Coast Reserve LTER 1989-present. Virginia Coast Reserve Long-Term Ecological Research Project Data Publication knb-lter-vcr.25.30 (http://metacat.lternet.edu/knb/metacat/knb-lter-vcr.25.30/lter).

Porter, J., D. Krovetz, J. Spitler, T. Williams, and K. Overman. 2014. Tide data for Hog Island (1991-), Redbank (1992-), Oyster (2007-). 12 minute interval. Virginia Coast Reserve Long-Term Ecological Research Project Data Publication knb-lter-vcr.61.22 (http://metacat.lternet.edu/knb/metacat/knb-lter-vcr.61.22/lter).

Raupach, M.R., Gillette, D.A., and Leys, J.F. 1993. The effect of roughness elements on wind erosion threshold. Journal of Geophysical Research 98 (D2): 3023-3029.

Ruggiero, P., Komar, P.D., McDougal, W.G., Marra, J.J., and Beach, R.A. 2001. Wave Runup, Extreme Water Levels, and the Erosion of Properties Backing Beaches. Journal of Coastal Research 17 (2): 407-419.

Schmidt, M. and Lipson, H. 2009. Distilling free-form natural laws from experimental data. Science 324 (5923): 81-85. doi: 10.1126/science.1165893

Seabloom, E.W., Ruggiero, P., Hacker, S.D., Mull, J., and Zarnetske, P.L. 2013. Invasive grasses, climate change, and exposure to storm-wave overtopping in coastal dune ecosystems. Global Change Biology 19: 824-832.

Seneca, E.D. 1972. Seedling response to salinity in four dune grasses from the outer banks of North Carolina. Ecology 53: 465-471.

Smiles, D.E. and Stokes, A.N. 1976. Periodic solutions of a nonlinear diffusion equation used in groundwater flow theory: examination using a Hele-Shaw model. Journal of Hydrology, 31: 27--35.

Stallins, J.A. 2002. Dune plant species diversity and function in two barrier island biogeomorphic systems. Plant Ecology 165: 183-196.

Stallins, J.A. 2005. Stability domains in barrier island dune systems. Ecological Complexity 2: 410-430.

Stalter, R. and Lamont, E.E. 1990. The vascular flora of Assateague Island, Virginia. Bulletins of the Torrey Botanical Club 117: 48-56.

Stalter, R., Tamory, J., Lynch, P., and Lockwood, B. 1999. The vascular flora of Biscayne National Park, Florida. Sida 18 (4): 1207-1226.

Tabacchi, E., Lambs, L., Guilloy, H., Planty-Tabbachi, A.M., Muller, E., and Decamps, H. 2000. Impacts of riparian vegetation on hydrological processes. Hydrological Processes 14 (16-17): 2959-2976.

Thom, B.G. and Hall, W. 1991. Behaviour of beach profiles during accretion and erosion dominated periods. Earth Surface Processes and Landforms 16: 113-127.

Travis, R. 1977. The effects of aspect and exposure on the growth of dune grasses in Cape Hatteras National Seashore. International Journal of Biometeorology 21 (3): 217-226.

United States Department of Labor. 2014. Inflation Calculator. Bureau of Labor Statistics.

Urish, D. W. and McKenna, T. E. 2004, Tidal effects on ground water discharge through a sandy marine beach. Groundwater 42: 971–982. doi: 10.1111/j.1745-6584.2004.tb02636.x

van der Valk, A.G. 1974. Environmental factors controlling the distribution of forbs on coastal foredunes in Cape Hatteras National Seashore. Canadian Journal of Botany 52: 1057-1073.

van Enckevort, I.M.J., Ruessink, B.G., Coco, G., Turner, I.L., Plant, N.G. et al. 2001. Observations of nearshore crescentic sandbars. Journal of Geophysical Research-Oceans 109 (C06028): 1-17. doi: 10.1029/2003JC002214.

Vick, J.K. and Young, D.R. 2011. Spatial variation in environment and physiological strategies for forb distribution on coastal dunes. Journal of Coastal Research 27 (6): 1113-1121.

Wilson, J.B. and Sykes, M.T. 1999. Is zonation on coastal sand dunes determined primarily by sand burial or by salt spray? A test in New Zealand dunes. Ecology Letters 2: 233-236.

Wolner, C.W.V., Moore, L.J., Young, D.R., Brantley, S.T., Bissett, S.N., and McBride, R.A. 2013. Ecomorphodynamic feedbacks and barrier island response to disturbance: Insights from the Virginia barrier islands, Mid-Atlantic bight, USA. Geomorphology 199 (1): 115-128.

Woodhouse, W.W., Seneca E.D., and Broome, S.W. 1977. Effect of Species on Dune grass growth. International Journal of Biometeorology 21 (3): 256-266.

Woodhouse, W.W. 1982. Coastal sand dunes of the U.S. In Lewis, R.R. (ed.). Creation and restoration of coastal plant communities. CRC Press: Boca Raton, FL, 1-44.

Wyatt, V.E. and Nickling, W.G. 1997. Drag and shear stress partitioning in sparse desert creosote communities. Canadian Journal of Earth Sciences 34: 1486 .

Young, D.R., Brantley, S.T., Zinnert, J.C., and Vick, J.K. 2011. Landscape position and habitat polygons in a dynamic coastal environment. Ecosphere 2 (6). doi: 10.1890/ES10-00186.1.

Zarnetske P.L., Hacker, S.D., Seabloom, E.W., Ruggiero, P., Killian, J.R. et al. 2012. Biophysical feedback mediates effect of invasive grasses on coastal dune shape. Ecology 93: 1439-1450.